Dosimetric effects caused by couch tops and immobilization devices: Report of AAPM Task Group 176

Arthur J. Olch[a)]
Radiation Oncology Department, University of Southern California and Children's Hospital Los Angeles, Los Angeles, California 90027

Lee Gerig
Department of Physics, Ottawa Hospital Regional Cancer Centre, Carleton University, Ottawa, Ontario K1S 5B6, Canada and Faculty of Medicine, University of Ottawa, Ottawa, Ontario K1N 6N5, Canada

Heng Li
Department of Radiation Physics, UT MD Anderson Cancer Center, Houston, Texas 77030

Ivaylo Mihaylov
Department of Radiation Oncology Department, University of Miami, Miami, Florida 33136

Andrew Morgan
The Beacon Centre, Musgrove Park Hospital, Taunton TA1 5DA, England

The dosimetric impact from devices external to the patient is a complex combination of increased skin dose, reduced tumor dose, and altered dose distribution. Although small monitor unit or dose corrections are routinely made for blocking trays, ion chamber correction factors, e.g., accounting for temperature and pressure, or tissue inhomogeneities, the dose perturbation of the treatment couch top or immobilization devices is often overlooked. These devices also increase skin dose, an effect which is also often ignored or underestimated. These concerns have grown recently due to the increased use of monolithic carbon fiber couch tops which are optimal for imaging for patient position verification but cause attenuation and increased skin dose compared to the "tennis racket" style couch top they often replace. Also, arc delivery techniques have replaced stationary gantry techniques which cause a greater fraction of the dose to be delivered from posterior angles. A host of immobilization devices are available and used to increase patient positioning reproducibility, and these also have attenuation and skin dose implications which are often ignored. This report of Task Group 176 serves to present a survey of published data that illustrates the magnitude of the dosimetric effects of a wide range of devices external to the patient. The report also provides methods for modeling couch tops in treatment planning systems so the physicist can accurately compute the dosimetric effects for indexed patient treatments. Both photon and proton beams are considered. A discussion on avoidance of high density structures during beam planning is also provided. An important aspect of this report are the recommendations the authors make to clinical physicists, treatment planning system vendors, and device vendors on how to make measurements of surface dose and attenuation and how to report these values. For the vendors, an appeal is made to work together to provide accurate couch top models in planning systems. © 2014 American Association of Physicists in Medicine. [http://dx.doi.org/10.1118/1.4876299]

Key words: carbon fiber couch top, immobilization device, surface dose, couch model

TABLE OF CONTENTS

1. INTRODUCTION

Radiotherapy patients are not treated suspended in mid-air, but often the treatment planning process proceeds as if they are. The dosimetric impact from devices external to the patient is a complex combination of increased skin dose, reduced tumor dose, and altered dose distribution; the magnitude being a function of beam energy, relative geometry of the beam and devices, the fraction of dose delivered through these devices, and their physical composition. Devices remote from the patient act primarily as attenuators and scatterers. Devices close to the patient act like bolus, increasing the skin dose and shifting the depth dose curve toward the patient surface. The overall effect can often be clinically significant as will be described in this report.

Maximizing radiotherapy outcomes generally demands dose delivery accurate to within 3% to 5% based on theoretical radiobiology considerations.[1–3] Using modern dosimetry protocols such as TG-51,[4] calibration uncertainty is 1% to 2% (for k = 1) while modern calculation methods have substantially improved treatment planning dose calculation accuracy. Many centers routinely make small (typically 2%–4%) monitor unit (MU) corrections for dose perturbations

caused by blocking trays, and to account for tissue inhomogeneities using the treatment planning system (TPS), even in tissue and bone where the correction is only a few percent. Temperature and pressure corrections to ion chamber readings and making the change to TG-51 calibration methods are two other examples of routine efforts to apply 1% to 2% dose corrections. While it is routine to address these small corrections, many in the radiotherapy community ignore the potentially larger dosimetric effects of devices such as couch tops and immobilization systems. This oversight is probably historical since there have rarely been accurate or practical ways of incorporating these devices into dose calculations and vendor-supplied data on the dosimetric impact of their devices has generally been inadequate. For beams perpendicular to a uniform slab, attenuation correction factors can be measured and applied manually to the MU calculation. However, for beams passing obliquely through nonuniform portions of the device, it is difficult to accurately account for these in manual MU calculations. The ability for TPS dose calculation algorithms to consider these devices is either not present or much more frequently, not implemented by the user. As with the other situations listed above where dosimetric corrections are regarded as necessary, dosimetric perturbations caused by devices external to the patient such as the couch top and immobilization devices should be included in dose calculations whenever possible.

Primarily driven by imaging considerations [Image Guided Radiotherapy (IGRT) and Cone Beam CT (CBCT)], modern couch tops are of a carbon fiber sandwich design; two thin carbon fiber plates each 2 mm to 4 mm thick sandwiching an air-equivalent polymeric foam or resin-impregnated paper honeycomb material. Carbon fiber materials are desirable due to their high mechanical strength, low specific density, and relative radio-translucence as first reported by de Mooy.[5] Although less attenuating than conventional solid couch tops which typically also incorporate solid metal rails, these new couch tops produce greater skin dose and dose attenuation than the older tennis racket inserts on conventional couch tops.[6]

The dosimetric effects of external devices (increased skin dose and reduced tumor dose) have been reported in the literature dating back to at least 1982.[7] Our literature search (completed in 2012) found 13 papers in the 1990s on this topic but that number grew quickly as the prevalence of carbon fiber couches and immobilization devices in the clinic increased. Since 2000, we identified 53 papers on this subject, 25 of them being published in 2009–2011. In many cases, the detailed dosimetric findings of the investigators have been at variance with the properties stated by the manufacturers. These references are found in Tables I and II and throughout this report.

With the introduction of volumetric modulated arc therapy (VMAT), a significant portion of the target dose is delivered through the couch top (and rails when present), creating a renewed interest in evaluating dose perturbations such as attenuation, increased skin dose, and target coverage effects. This report provides a literature review of the dosimetric effects

TABLE I. Surface dose by type of external device and delivery method.

Device	Delivery type	Beam angle(s)	Depth on surface (cm)	Surface dose in% of d_{max}/open field dose in% of d_{max} (energy)	Detector type	Study reference
Carbon fiber grid tabletop (Varian)	Single beam	0°[a] 15°[b] 30°[b] 45°[b] 60°[b]	0.015	32%/19% (6 MV) 38%/19% (6 MV) 41%/19% (6 MV) 49%/19% (6 MV) 62%/19% (6 MV)	Ion chamber parallel-plate (Attix) EBT Gafchromic film	Butson *et al.* (Ref. 24)
Carbon fiber insert (Sinmed)	Single beam	Normal incidence	0.0 0.0	68%/18% (8 MV)	Ion chamber parallel-plate (PTW)	Higgins *et al.* (Ref. 19)
Carbon fiber tabletop (Medtec)	Single beam	180°[a]	0.05	77%/17% (6 MV) 49%/10% (18 MV)	Ion chamber parallel-plate (PTW, Scanditronix)	Gerig *et al.* (Ref. 13)
Carbon fiber tabletop (Medical Intelligence)		180°[a]		89%/17% (6 MV) 75%/13% (10 MV)		
iBEAM Carbon fiber tabletop (Medical Intelligence)	Single beam	0°[a] 60°[b] 0°[a] 60°[b]	0.0	92%/18% (6 MV) 98%/34% (10 MV) 78%/13% (6 MV) 92%/27% (10 MV)	EBT Gafchromic film	Smith *et al.* (Ref. 66)
Carbon fiber tabletop + vacuum immobilization device	IMRT single fraction	5-field/2 posterior	0.0	58%/NA (10 MV)	TLD	Lee *et al.* (Ref. 47)
Contessa tabletop Candor Aps	Single beam	0°[a]	0.5	97%/83% (6 MV) 79%/59% (18 MV)	Ion chamber parallel-plate (PTW)	Berg *et al.* (Ref. 23)
Contessa tabletop + breastboard Candor Aps		0°[a]		100%/83% (6 MV) 93%/59% (18 MV)		
Carbon fiber tabletop (Reuther Medizintechnik)	Single beam	180°[a] 150°[b]	0.1	92%/51% (6 MV) 80%/36% (10 MV) 94%/51% (6 MV) 84%/36% (10 MV)	Ion chamber parallel-plate (PTW)	Poppe *et al.* (Ref. 55)
Carbon fiber tabletop + combiboard		180°[a] 150°[b]		98%/51% (6 MV) 93%/36% (10 MV) 99%/51% (6 MV) 95%/36% (10 MV)		
Carbon fiber Mylar insert (Varian) Carbon fiber tennis string insert (Varian)	Single beam	0°[a] 0°[a]	0.017	48%/16% (6 MV) 35%/16% (6 MV)	Gafchromic film	Butson *et al.* (Ref. 24)
Elekta C-arm tabletop	Single beam	180°[a]	0.1	38%/28% (6 MV) 20%/16% (18 MV)	EDR2 radiographic film	Gillis *et al.* (Ref. 38)
Sinmed Mastercouch		180°[a]		74%/28% (6 MV) 48%/16% (18 MV)		
Sinmed Mastercouch + support bar		180°[a]		83%/28% (6 MV) 62%/16% (18 MV)		
Carbon fiber grid with mylar sheet	Single beam	180°[a]	0.015	26%/20% (6 MV)	EBT radiochromic film (Ref. 56)	Chiu-Tsao and Chan
Orfit carbon fiber base plate Balsa wood board Styrofoam Aqua-plast sheet Alpha-cradle				71%/20% (6 MV) 69%/20% (6 MV) 55%/20% (6 MV) 38%/20% (6 MV) 45%/20% (6 MV)		
PMMA 12.5 mm plate	Single beam	0°[a]	0.0	100%/18% (Co-60) 83%/21% (6 MV) 74%/20% (23 MV)	Ion chamber parallel-plate (Markus)	De Ost *et al.* (Ref. 18)
Wood		0°[a]		100%/18% (Co-60) 82%/21% (6 MV) 73%/20% (23 MV)		
Carbon1 Orfit		0°[a]		74%/18% (Co-60) 49%/21% (6 MV)		

TABLE I. *(Continued).*

Device	Delivery type	Beam angle(s)	Depth on surface (cm)	Surface dose in% of D_{max}/open field dose in% of d_{max} (energy)	Detector type	Study reference
Carbon2 Orfit		0°[a]		29%/20% (23 MV) 77%/18% (Co-60) 55%/21% (6 MV)		
Carbon3 Sinmed		0°[a]		34%/20% (23 MV) 76%/18% (Co-60) 51%/21% (6 MV)		
Carbon fiber 1.1 cm		Normal incidence	0.0	32%/20% (23 MV) 64%/19% (4 MV) 50%/15% (6 MV) 38%/11% (10 MV)	Ion chamber parallel-plate (NACP)	Carl and Vestergaard (Ref. 29)
Carbon fiber 4.1 cm				82%/19% (4 MV) 66%/15% (6 MV) 53%/11% (10 MV)		
Polystyrene cradle 1.0 cm				51%/19% (4 MV) 41%/15% (6 MV) 30%/11% (10 MV)		
Polystyrene cradle 4.0 cm				66%/19% (4 MV) 56%/15% (6 MV) 42%/11% (10 MV)		
Thermoplastic material 0.15 cm				39%/19% (4 MV)[c] 30%/15% (6 MV)[c] 22%/11% (10 MV)[c]		
Thermoplastic material 0.2 cm				49%/19% (4 MV)[c] 40% / 15% (6 MV)[c] 28%/11% (10 MV)[c]		
Carbon fiber composite slab	Single beam	180°[a]	0.004	59%/18% (5 MV) 56% / 15% (6 MV) 43%/12% (8 MV)	Ion chamber parallel-plate (Vinten)	Meara and Langmack (Ref. 48)
PMMA baseboard				98%/18% (5 MV) 98%/15% (6 MV) 93%/12% (8 MV)		
PETG copolyester				78%/18% (5 MV) 75%/15% (6 MV) 62%/12% (8 MV)		
Thermoplastic immobilization devices	Single beam	Normal incidence	0.0	60%/17% (6 MV)[c] 40%/11% (15 MV)[c]	Ion chamber parallel-plate (Attix)	Hadley *et al.* (Ref. 50)
Thermoplastic immobilization devices	Single beam	Normal incidence	0.05	77%/57% (Co-60) 63%/49% (4 MV) 63%/49% (6 MV)	TLD	Halm *et al.* (Ref. 51)
Thermoplastic immobilization (Med-Tec)	IMRT	7-field	0.0	152 cGy /125 cGy (6 MV) (with/without mask)	TLD	Lee *et al.* (Ref. 31)
Aquaplast solid 0.3 cm	Single beam	Normal incidence	0.1	80%/24% (6 MV)[c] 58%/19% (15 MV)[c]	Ion chamber parallel-plate (Holt)	Fontenla *et al.* (Ref. 52)
Thermoplastic mask	Single beam	Normal incidence	0.0	36%/15% (6 MV) 24%/12% (15 MV)	Ion chamber parallel-plate (PTW)	Mellenberg (Ref. 45)
Immobilization cradle (polyurethane)				63%/15% (6 MV)[c] 47%/12% (15 MV)[c]		
Immobilization cradle (polystyrene)				66%/15% (6 MV) 45%/12% (15 MV)		
Thermoplastic immobilization devices	Single beam	Normal incidence			Ion chamber parallel-plate (Markus)	Fiorino *et al.* (Ref. 53)
Orfit Raycast 0.2 cm			0.0	56%/16% (6 MV)		
Orfit Raycast 0.32 cm			0.0	74%/16% (6 MV)		
Optimold 0.24 cm			0.0	62%/16% (6 MV)		
Optimold 0.32 cm			0.0	67%/16% (6 MV)		

TABLE I. *(Continued).*

Device	Delivery type	Beam angle(s)	Depth on surface (cm)	Surface dose in% of D_{max}/open field dose in% of d_{max} (energy)	Detector type	Study reference
Vacuum compressed immobilization device (Vacbag)	Single beam	Normal incidence	0.01	52%/16% (6 MV)	Ion chamber parallel-plate (Attix)	Cheung *et al.* (Ref. 46)
Polyurethane-foam immobilization devices	Single beam	Normal incidence	0.0	91%/28% (Co-60)[c]	Ion chamberparallel-plate (Capintec)	Mondalekal (Ref. 7)
				76%/20% (4 MV)[c]		
				48%/13% (10 MV)[c]		
				38%/10% (15 MV)[c]		
Immobilization devices	Single beam	Normal incidence	0.0		Ion chamber parallel-plate (Capintec)	Johnson *et al.* (Ref. 44)
Alpha Cradle				81%/28% (Co-60)[c]		
				51% / 17% (6 MV)[c]		
				31%/14% (18 MV)[c]		
VacFix				89%/28% (1.2 MV)[c]		
				58%/17% (6 MV)[c]		
				35%/14% (18 MV)[c]		
Silicon-based burn dressing	Single beam	Normal incidence	0.1	50.5%/16% (6 MV)	Ion chamber parallel-plate (Attix) TLD EBT Gafchromic film	Butson *et al.* (Ref. 25)
Brainlab	Single beam (10 × 10)	Normal incidence	0.06	98.6%/44.3% (6 MV)	Plane parallel chamber NACP-02 (uncorrected)	Seppälä and Kulmala (Ref. 6)
Qfix kVue standard				88.5%/44.3% (6 MV)		
Medtec				90.1%/44.3% (6 MV)		
Varian Exact IGRT				90.8%/44.3% (6 MV)		
Dignity Airplate				86.0%/44.3% (6 MV)		
Qfix DoseMax				75.1%/44.3% (6 MV)		
Varian Grid insert				61.2%/44.3% (6 MV)		

[a]Posterior.
[b]Posterior oblique.
[c]Variable with stretching/thickness.

of couch tops and immobilization devices, including dosimetry data for many commonly available devices and linacs. It does not address devices such as bolus, blocks or wedges that are deliberately introduced to modify dose. The magnitude of the dosimetric effects caused by particular devices in low and high energy beams is given as well as guidance on the measurements required by the physicist and how these measurements may be made.

Target localization systems such as the Calypso system introduce devices which the beam may pass through but are not present in the planning CT images. The dosimetric effects of this system are discussed.

In CT-based planning, the CT couch top is typically part of the patient image. Although the linac couch top may attenuate the beam by up to 15% (see Table II), before around 2008, it was difficult to include it in TPS dose calculations. Many current TPS software releases still do not provide the means to replace the CT couch top with the actual treatment couch top, however, from its earliest version, the TomoTherapy (Accuray, Sunnyvale, CA) planning software has implemented this. Varian has recently implemented software to automatically insert certain Varian couch tops under the patient to increase the accuracy of the dose calculations.[8–10] Other treatment planning systems have also begun to offer methods to directly include the treatment couch top in the planning CT while others can accept modified CT datasets.[11–14] These methods will be discussed in more detail later in the report as well as guidance on the creation of plans in which beams largely miss external structures and on methods that predict when beams will pass through these structures.

Dose perturbation due to the couch top may vary if the position of the patient relative to the couch top varies day to day, making a single compensatory solution potentially inaccurate. Indexed patient immobilization systems are now commonly used to establish reproducible patient position relative to the couch and employing such devices provides the best opportunity to accurately account for the couch top (and rails if present) during the planning process. The recommendations in this report will be most relevant to the

TABLE II. Attenuation for patient support couches and/or immobilization devices.

Device	Delivery type	Beam angle(s)	Attenuation (energy)	Detector type	Study reference
Metallic centerspine bar for Clinac 4/100 couch	Conformal arc	0°[a] to 60°[b]	8%–12% (4 MV)	XV film/ion chamber cylindrical (PTW)	Krithivas and Rao (Ref. 35)
Carbon fiber tabletop (Reuther MedizinTechnik)	Single beam	180°[a] 120°[b]	3.0% (6 MV) 2.0% (18 MV) 5.6% (6 MV) 4.0% (18 MV)	Ion chamber cylindrical PTW	Meydanci and Kemikler (Ref. 32)
ExacTrac IGRT tabletop (BrainLab)	Single beam	0°[a] 30°[b] 50°[b] 75°[b] 83°[b]	3.0% (6 MV) 0.1% (18 MV) 3.2% (6 MV) 0.6% (18 MV) 5.6% (6 MV) 2.6% (18 MV) 8.7% (6 MV) 5.0% (18 MV) 5.3% (6 MV) 2.9% (18 MV)	Ion chamber cylindrical (PTW)	Mihaylov *et al.* (Ref. 14)
Carbon fiber tabletop (Medtec)	Single beam	180°[a] 160°[b] 140°[b] 120°[b] 100°[b]	1.2% (6 MV) 1.4% (6 MV) 1.9% (6 MV) 3.0% (6 MV) 0.01% (6 MV)	Ion chamber cylindrical (Wellhofer)	Munjal *et al.* (Ref. 57)
Carbon fiber tabletop (Medtec)	Single beam	225°[b]	6.8% (6 MV) 4.7% (18 MV)	Ion chamber cylindrical Farmer	Myint *et al.* (Ref. 37)
IGRT tabletop (Siemens)	Single beam	180°[a] 150°[b]	2.4% (6 MV) 4.6% (6 MV)	Ion chamber cylindrical pinpoint	Spezi and Ferri (Ref. 22)
IGRT tabletop (Varian)	Single beam	180°[a] 225°[b]	3.1% (6 MV) 2.0% (15 MV) 4.4% (6 MV) 3.0% (15 MV)	Ion chamber array (PTW)	Vanetti *et al.* (Ref. 8)
	modulated arc (Varian)		1.9% (6 MV) 1.3% (15 MV)	TPS calculations	
Exact tabletop (Varian)	Single beam	Carbon fiber inserts[a] couch rails[b]	3.0% (6 MV) 15.0% (6 MV)	EPID/Ion chamber cylindrical	Vieira *et al.* (Ref. 73)
Carbon fiber tabletop (Medtec)	Single beam	115°[b] 120°[b] 125°[b] 115°[b] 120°[b] 125°[b]	5.5% (6 MV) 5.0% (6 MV) 6.5% (6 MV) 4.0% (18 MV) 3.3% (18 MV) 4.3% (18 MV)	Ion chamber cylindrical	Gerig *et al.* (Ref. 13)
Carbon fiber tabletop (Medical Intelligence)		120°[b] 125°[b] 130°[b] 120°[b] 125°[b] 130°[b]	3.4% (6 MV) 4.0% (6 MV) 3.9% (6 MV) 2.7% (10 MV) 3.3% (10 MV) 3.2% (10 MV)		
iBEAM Carbon fiber tabletop (Medical Intelligence)	Single beam	0°[a] 50°[b] 0°[a] 50°[b]	2.7% (6 MV) 4.6% (6 MV) 1.9% (10 MV) 4.0% (10 MV)	Ion chamber cylindrical	Smith *et al.* (Ref. 66)
Varian Exact couch and rail	Single beam	180°[a] 240°[b]	1%–17% (6 MV)	Ion chamber cylindrical	Van Prooijen *et al.* (Ref. 41)
Sinmed		180°[a]	2.5%–16%(6 MV)		

TABLE II. *(Continued).*

Device	Delivery type	Beam angle(s)	Attenuation (energy)	Detector type	Study reference
Mastercouch and wedged section		240°[b]	2.2%–14% (10 MV) 1.6%–11% (18 MV)		
Sinmed BV Posisert insert	Single beam	180°[a] 110°[b]	2.2% (6 MV) 8.7% (6 MV)	Ion chamber cylindrical (PTW)	McCormack *et al.* (Ref. 21)
Contessa tabletop Candor Aps	Single beam	0°[a] 60°[b] 75°[b]	2.0% (6 MV) 1.3% (18 MV) 4.8% (6 MV) 2.9% (18 MV) 5.5% (6 MV) 3.4% (18 MV)	Ion chamber cylindrical Farmer	Berg *et al.* (Ref. 23)
Contessa tabletop + breastboard Candor Aps		0°[a] 60°[b] 75°[b]	3.5% (6 MV) 1.9% (18 MV) 8.0% (6 MV) 5.2% (18 MV) 5.3% (6 MV) 3.5% (18 MV)		
Elekta stereotactic body frame + table	Single beam	180°[a] 215°[b] 246°[b] 270° 284°	6.9% (6 MV) 4.8% (16 MV) 10.6% (6 MV) 7.0% (16 MV) 5.8% (6 MV) 4.0% (16 MV) 6.8% (6 MV) 4.8% (16 MV) 9.4% (6 MV) 5.5% (16 MV)	Ion chamber cylindrical (Exradin A16)	Becker *et al.* (Ref. 59)
Carbon fiber tabletop (Reuther Medizintechnik)	Single beam	180°[a] 150°[b]	2.7% (6 MV) 2.3% (10 MV) 3.2% (6 MV) 2.4% (10 MV)	Ion chamber parallel-plate (PTW)	Poppe *et al.* (Ref. 55)
Carbon fiber tabletop + combiboard		180°[a] 150°[b]	5.2% (6 MV) 4.1% (10 MV) 6.4% (6 MV) 4.9% (10 MV)		
Patient support assembly centerspine bar	Conformal arc	0°[a] to 359°[b]	2.9% (6 MV) 1.8% (18 MV)	Ion chamber cylindrical Farmer	Sharma and Johnson (Ref. 36)
Patient support assembly side rails			2.9% (6 MV) 2.4% (18 MV)		
Elekta C-arm tabletop	Single beam	180°[a]	0.3% (6 MV) 0.2% (18 MV)	Ion chamber cylindrical Farmer	Gillis *et al.* (Ref. 38)
Sinmed Mastercouch		180°[a]	1.5% (6 MV) 1.5% (18 MV)		
Sinmed Mastercouch + support bar		180°[a]	3.7% (6 MV) 2.4% (18 MV)		
Carbon fiber composite slab	Single beam	180°[a]	0.8% (5 MV) 0.5% (6 MV) 0.4% (8 MV)	Ion chamber cylindrical Farmer	Meara and Langmack (Ref. 48)
PMMA baseboard			4.3% (5MV) 3.7% (6 MV) 3.2% (8 MV)		
PETG copolyester			1.2% (5MV) 1.4% (6 MV) 1.2% (8 MV)		

TABLE II. *(Continued)*.

Device	Delivery type	Beam angle(s)	Attenuation (energy)	Detector type	Study reference
PMMA 12.5 mm plate	Single beam	0°[a]	5.0% (Co-60)	Ion chamber parallel-plate (Markus)	De Ost *et al.* (Ref. 18)
			4.0% (6 MV)		
			2.0% (23 MV)		
Wood		0°[a]	5.0% (Co-60)		
			4.0% (6 MV)		
			2.0% (23 MV)		
Carbon1 Orfit		0°[a]	0.0% (Co-60)		
			0.0% (6 MV)		
			0.0% (23 MV)		
Carbon2 Orfit		0°[a]	1.0% (Co-60)		
			1.0% (6 MV)		
			0.0% (23 MV)		
Carbon3 Sinmed		0°[a]	1.0% (Co-60)		
			0.0% (6 MV)		
			0.0% (23 MV)		
Carbon fiber head fixation	Single beam	Base plate[a]	4.0% (6 MV	Diode	Olch and Lavey (Ref. 49)
VBH HeadFix		Vertical posts[a]	15.0% (6 MV)		
Polyurethane-foam immobilization devices	Single beam	Normal incidence	1.7% (Co-60)[c]	Ion chamber parallel-plate (Capintec)	Mondalek (Ref. 7)
			1.6% (4 MV)[c]		
			1.1% (10 MV)[c]		
			1.0% (15 MV)[c]		
Brainlab	Single beam	Normal incidence	3.6% (6 MV)	Ion chamber (NE-2571)	Seppälä and Kulmala (Ref. 6)
Qfix kVue standard			2.1% (6 MV)		
Medtec			1.9% (6 MV)		
Varian Exact IGRT			1.9% (6 MV)		
Dignity Airplate			1.9% (6 MV)		
Qfix DoseMax			1.3% (6 MV)		
Varian Grid insert			0.3% (6 MV)		

[a]Posterior.
[b]Posterior oblique.
[c]Variable with stretching/thickness.

situation of the indexed patient, but will apply more generally as well.

Although the majority of this report is concerned with photon beams, charged particle therapy is potentially even more impacted by external devices which partially use the finite particle range, potentially causing substantially underdosed regions in the distal portions of the PTV. Most electron beam treatments are single en-face fields that directly irradiate the patient, but proton beam therapy is often optimized using beams from different directions, some of which can intersect the couch top and immobilization devices. This report also discusses the dosimetric impact of these devices on proton beams.

A review of current limitations of commonly used TPSs reveals some of the practical problems encountered when including all sources of beam perturbation in the dose calculation. This report provides recommendations to TPS vendors regarding features that should be included in TPS software to allow the accurate inclusion of all external structures that affect dose. Recommendations are also made to couch top and immobilization device vendors to provide attenuation and surface dose data for limited but defined irradiation conditions as well as detailed information about the structure and material composition of each device.

2. DOSIMETRIC EFFECTS OF EXTERNAL DEVICES

2.A. Couch tops

2.A.1. Impact on skin dose

From the early days of radiotherapy, skin was used as a "dosimeter" (erythema dose) and there is a significant knowledge base for skin dose-response. Archambeau *et al.* provides an excellent discussion of the pathophysiology, anatomy, and dose response of the skin, describing clinically observed skin and hair changes as a function of total dose and fraction size. Skin doses over about 25 Gy at 2 Gy per fraction produce clinically relevant skin reactions and greater than 45 Gy may produce dry desquamation.[15] The radio-sensitivity of the skin is often enhanced by concomitant chemotherapy or near sites of surgical intervention while larger doses per fraction, commonly used in stereotactic radiotherapy, exacerbate the skin reaction for the same total dose.[16] In this report, the term

"surface dose" is used to describe the dose to an infinitesimal mass at the very surface of a phantom, while "skin dose" is a clinical term and refers to the dose to the radiation sensitive epithelial layer.

There are many well-known clinical situations where skin dose can be excessive (e.g., skin folds, electron or orthovoltage beams, bolus). However, the impact of couch tops and immobilization devices is often not well recognized. Kry *et al.* recently presented a review of all factors affecting skin dose in radiotherapy.[17] Interestingly, there are more physics-based reports on the potential loss of skin sparing from external devices than clinical reports on skin toxicity due to those devices. This disparity does not necessarily mean clinically relevant skin reactions are not occurring; they may be underreported or other mitigating factors are at work, such as the use of multiple beams reducing the dose to any one part of the skin.

Numerous publications show a significant increase in surface dose when beams first transit carbon fiber couch tops at either normal or oblique incidence[6,18–24] and show these to be larger than for the mylar-covered tennis racket couch top[25] (Table I). While there is some consistency in the methodology used for measuring and reporting the dose attenuation, there are large variations in the methodology used to determine and report the surface dose. One must be cautious when interpreting reported surface doses because the dose gradient at the surface is very steep at approximately 2% for every 0.1 mm so that the true depth at which the "surface" dose is reported becomes critical (see Tables III–V). In our literature review, various authors reported the "surface" dose of 13% up to 83% for depths ranging from 0 to 0.5 cm for (typically 10 × 10 cm^2) 6 MV x-rays compared to accurate estimates of surface dose of about 16% (Table V). Errors in the measurement of

TABLE III. PDD for 6 MV x-rays in the buildup region (data measured with an Attix parallel plate chamber, adapted from data provided by Michael Evans, McGill University, Montreal, Canada).

	6 MV buildup PDD Square field size (cm)						
Depth (mm)	4	6	8	10	15	20	30
0	9	11	14	16	22	28	40
1	33	35	37	39	44	49	59
2	52	53	55	56	61	64	72
3	65	66	67	69	72	75	80
4	74	75	76	77	79	82	85
5	81	82	82	83	85	86	88
6	85	86	87	87	88	89	90
7	89	89	90	90	91	91	92
8	91	92	92	92	93	93	93
9	93	94	94	94	95	95	95
10	95	95	96	96	97	97	97
11	97	97	97	97	99	99	99
12	98	98	99	99	99	100	100
13	99	100	100	99	99		
14	100	100	100	100	100		
15	100	100	100	100			

TABLE IV. PDD for 10 MV x-rays in the buildup region (data measured with an Attix parallel plate chamber, adapted from data provided by Michael Evans, McGill University, Montreal, Canada).

	10 MV buildup PDD Square field size (cm)						
Depth (mm)	4	6	8	10	15	20	30
0	7	8	10	13	19	24	34
1	24	25	27	30	35	39	49
2	38	40	41	43	48	52	60
3	50	51	52	55	58	62	70
4	60	61	62	64	67	70	77
5	68	69	69	71	74	77	82
6	74	75	76	77	79	82	86
7	79	80	80	82	84	86	90
8	83	84	84	85	87	89	92
9	86	87	87	88	90	91	94
10	89	89	90	91	92	93	95
11	91	91	92	92	94	95	96
12	92	93	93	94	95	96	97
13	94	94	94	95	96	97	98
14	95	95	96	96	97	98	99
15	96	96	97	97	98	99	100
16	97	97	98	98	99	99	
17	98	98	98	99	99	100	
18	99	99	99	99	100		
19	99	99	99	99			
20	99	99	100	100			
21	99	100					
22	100						

the unattenuated surface dose will generally carry over to the measurement for intervening devices. It should also be noted that field size dependence of surface dose (see Tables III–V) is considerably greater than that for attenuation. Table I details the reported surface doses for 24 studies for a wide variety of devices. The reported surface doses for the external devices should be understood in light of the open field surface dose and depth of measurement also listed.

To determine the clinical effect of surface dose it is important to consider the skin anatomy. Whitton reported the depth of the sensitive basal cell (growing) layer varies between 0.05 and 0.4 mm, depending on anatomical site.[26] The ICRU and ICRP recommend that skin dose be measured at 0.07 mm depth, which corresponds to the approximate depth of the basal cell layer.[27,28] A depth of 0.1 mm has frequently been used as a reasonable reference depth of the basal cell layer of skin.[29] Measurements made at an effective depth greater than the basal layer depth will overestimate the "skin dose." Carl and Vestergaard measured surface doses for beams passing through a variety of thermoplastic and carbon fiber devices and provided water equivalent thicknesses (WET) and normal tissue complication probability (NTCP) calculations of early and late skin damage for 4, 6, and 10 MV photon beams.[29]

The clinical importance of skin dose is often overlooked when treating with megavoltage photon beams, where the clinical goal is to eradicate deep seated tumors. However, clinically relevant skin toxicity due to the passage of beams

TABLE V. PDD for 18 MV x-rays in the buildup region (data measured with an Attix parallel plate chamber, adapted from data provided by Michael Evans, McGill University, Montreal, Canada).

Depth (mm)	18 MV buildup PDD Square field size (cm)						
	4	6	8	10	15	20	30
0	6	9	12	16	23	29	41
1	17	21	24	27	34	41	52
2	28	31	34	37	44	51	61
3	37	40	43	46	53	59	68
4	45	48	51	54	60	66	74
5	52	55	58	60	66	72	79
6	58	61	64	66	72	76	82
7	63	66	69	71	76	80	85
8	68	71	73	75	80	83	88
9	72	74	77	79	83	86	90
10	76	78	80	82	85	88	91
11	79	81	82	84	88	90	92
12	81	83	85	86	89	91	93
13	84	85	87	88	91	93	94
14	86	87	88	90	92	94	95
15	87	89	90	91	93	95	96
16	89	90	91	92	94	96	97
17	90	91	92	93	95	96	98
18	91	92	93	94	96	97	98
19	93	93	94	95	97	98	99
20	94	94	95	96	97	99	99
21	95	95	96	97	98	99	100
22	96	96	97	97	98	100	
23	96	97	98	98	99		
24	97	98	98	99	100		
25	98	98	99	99			
26	99	99	99	100			
27	99	99	100				
28	100	100					
29	100						
30							

through the couch top and immobilization devices has been reported in the literature.[16,30,31] Hoppe described one case of grade 4 skin toxicity in patients undergoing large dose per fraction stereotactic body radiotherapy using three posterior 6 MV beams passing through the treatment couch top and immobilization device (Fig. 1). The original plan failed to include these devices and led the planner to think the skin dose was about 50% while subsequent replanning simulating the inclusion of these devices revealed a 90% skin dose.[16] This skin reaction was due to a combination of too few (all posterior) beams, a target volume close to the skin surface, and the intervening external devices. However, inclusion of the intervening devices in the TPS dose calculation would have given the planner ample reason to question whether the skin dose was safe. It should be noted that increasing the MU to correct for couch attenuation will further increase the absolute skin dose.

Another clinical example, a medulloblastoma patient treated supine on an IGRT couch top, is shown in Fig. 2 (personal communication by author A. J. Olch). The prescribed dose was 23.4 Gy in 1.8 Gy fractions to the craniospinal axis. The spinal dose was prescribed to 5 cm depth using a PA field. Post treatment, a grade 2–3 skin reaction was observed on the patient's back, which was more prominent at the superior aspect of the spine field. The maximum superficial dose from this treatment was ≥29 Gy (2.2 Gy/fraction) and much of the increased skin dose was due to treatment through the carbon fiber couch top. Note that the planning system did predict the high dose region corresponding to the region of the worst aspect of the skin reaction superiorly but placed it at about 1 cm below the skin surface because the couch top was ignored.

Skin dose is influenced by both energy and field size. Figure 3 shows the surface dose is increased from about 10%–60% for 6 MV and 15%–75% for 18 MV (a 50%–60% *absolute* dose increase) for a 10×10 cm^2 field with and without the carbon fiber couch top.[32] Seppala and Kulmala measured the surface dose associated with 8 different couch tops for 6 MV and 15 MV photons for 10×10 cm^2 and
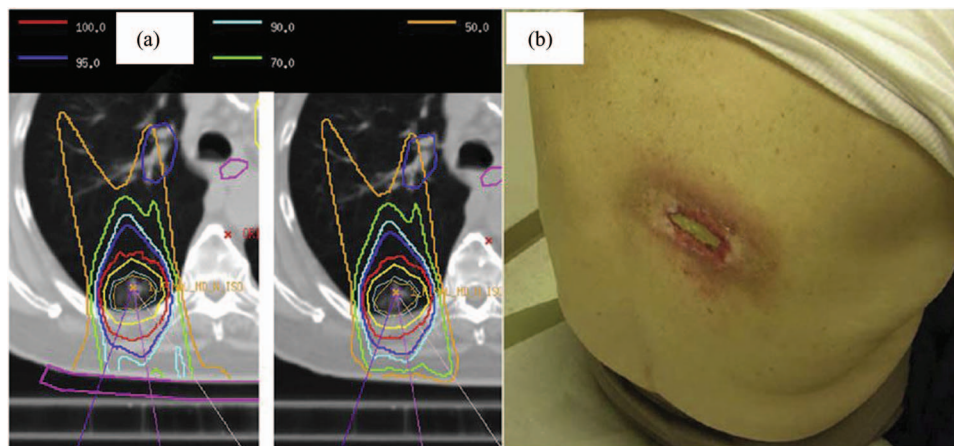

FIG. 1. (a) (Left panel) Isodoses after including simulated bolus; (right panel) original isodose distribution used to treat the patient. (b) Grade 4 skin reaction. From Hoppe *et al.*, "Acute skin toxicity following stereotactic body radiation therapy for stage I non-small-cell lung cancer: who's at risk?," Int. J. Radiat. Oncol., Biol., Phys. **72**, 1283–1286 (2008).
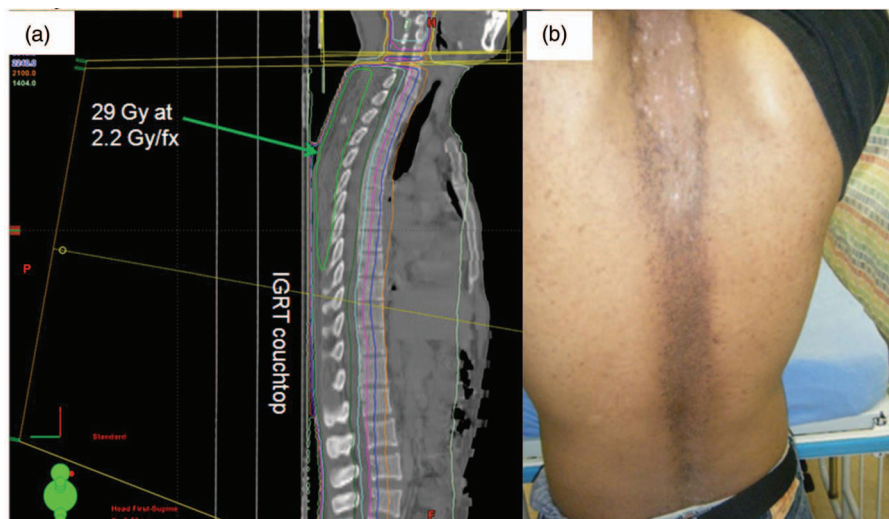
FIG. 2. (a) PA spine used in craniospinal irradiation (6 MV), 23.4 Gy to depth of 5 cm with spine field treating through carbon fiber couch top, couch angle was 90°, gantry was angled inferiorly. More than 29 Gy was delivered to the skin in the superior half of the spine field in the presence of the carbon fiber IGRT couch top but the TPS dose was less due to the absence of the couch top. (b) Skin reaction from treatment in (a).

20×20 cm^2 fields. Depending on the type of couch top, surface doses for a 10×10 cm^2 field increased by 26%–37.4% (*absolute*) for 6 MV and 20% to 43.5% (*absolute*) for 15 MV photons.[6]

The skin dose from external devices is also affected by the air gap between the device and the skin. As this air gap increases, lateral electron transport reduces the skin dose. Figure 4 shows a typical treatment setup where an air gap exists between a head and neck mask baseplate and the patient's posterior skin surface. Skin sparing was partially reestablished if the air gap was more than about 5 cm; the skin dose was reduced from 100% to either 90% or 62% with air gaps of 5 or 15 cm, respectively. The analytical anisotropic algorithm (AAA) (Varian Medical Systems, Palo Alto, CA) overestimated the depth of maximum dose in the secondary buildup region by about 2 to 5 mm and overestimated the dose at depth by up to 4% for the range of air gaps studied.[33]

Skin dose can also be an issue for modern treatment methods. For example, Mihaylov *et al.* showed that VMAT mixed energy posterior arcs (6 and 18 MV) resulted in lower skin dose than 6 MV arcs alone.[34]

2.A.2. Impact on attenuation

In addition to increasing skin dose, patient support and immobilization devices also attenuate the photon beam. Prior to carbon fiber couch tops, the most attenuating portion of most couches was the high Z center spine or side rails. Krithivas and Rao presented early work on the issue by examining the attenuation of a 4 MV beam by the center-spine of a Clinac 4/100 couch where 60° posterior arcs resulted in dose reductions of 8%–12%.[35] Sharma and Johnson expanded on this work, including attenuation due to couch side rails.[36]

For modern carbon fiber couch tops, attenuation of up to 15% can be seen for certain parts of the couch top with
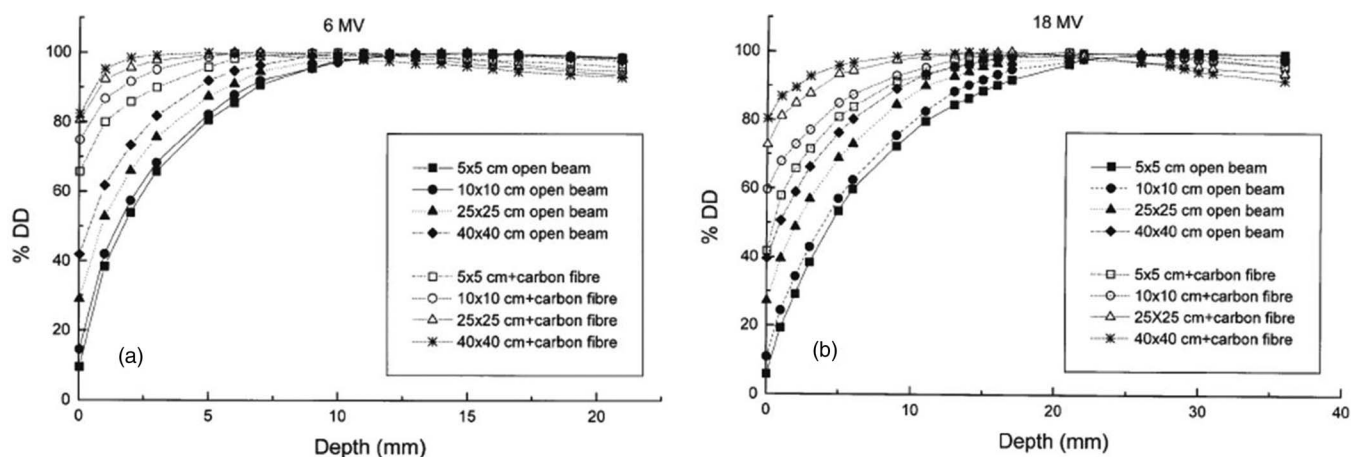

FIG. 3. PDD for 6 MV and 18 MV for different field sizes with and without couch top. From Meydanci and Kemikler, "Effect of a carbon fiber tabletop on the surface dose and attenuation for high-energy photon beams," Radiat. Med. **26**, 539–544 (2008).
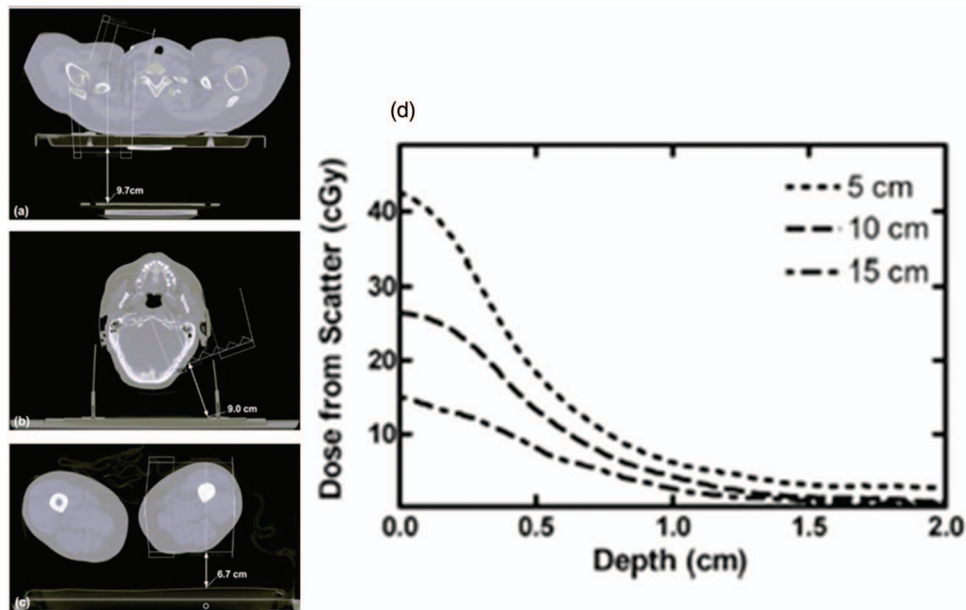
FIG. 4. (a)–(c) Three different scenarios where air gaps exist between immobilization devices or couch tops and the skin surface. (d) Dose at depth produced from scatter created by a 2 cm water equivalent slab positioned before 5, 10, and 15 cm air gaps (100 MU, 6 MV photon beams, 10×10 cm^2 field size, 100 cm SSD to the surface of the water phantom). From Gray *et al.*, "The accuracy of the pencil beam convolution and anisotropic analytical algorithms in predicting the dose effects due to attenuation from immobilization devices and large air gaps," Med. Phys. **36**, 3181–3191 (2009).

2%–5% being typical (Table II). As expected, attenuation increases with decreasing photon energy, increasing angle of incidence to the couch, and to a lesser extent, increasing field size. Most papers give attenuation data for just one field size, usually 10×10 cm^2. Myint *et al.* showed about a 1% difference in attenuation for 6 MV for 5×5 cm^2 vs 10×10 cm^2 when the magnitude of attenuation was 7% (through a strut).[37] Several reports showed that couch attenuation can increase 4-fold as the beam angle ranges from 0° to 70°.[14,21–23] As pointed out by McCormack *et al.*, manually correcting the central axis dose for this attenuation may lead to an overdose or underdose to regions of the patient where the beam transited a different part of the couch top.[21] This is demonstrated in Fig. 5 which shows the differential effect of dose perturbation for a 6 MV beam oblique to the couch top and partially subtended by it.

The variation in couch top attenuation as a function of beam angle is shown in Fig. 6. For 6 MV, attenuation of 1.2%–3.4% and 3.1%–8% was found for normal or 60° beam incidence, respectively.[23] In another study of 8 different couch tops, the absolute attenuation of a 6 MV beam varied by 3%–8% as the angle of incidence ranged from 90° to 180°.[6] A common conclusion from these studies is that carbon fiber couch tops which are ideal for imaging may not necessarily be ideal for treatment and that carbon fiber support structures, such as rails and frame sections in tennis racket style couch tops must be considered during treatment planning.[38]

Dose and dose distribution effects of excluding the couch top or rails from intensity modulated dose calculations have also been reported. For a RapidArc treatment with the couch not included in the dose calculation, Popple showed up to a 5.8% underdose at isocenter[39] and Vanetti *et al.* demonstrated

reduced PTV coverage. In other VMAT studies and for multi-beam fixed gantry IMRT plans, the measured dose at isocenter was reported to be 2% to 3% lower than the calculated dose when the couch and rails were ignored[9,10,40,41] Pulliam *et al.* studied the effects of the rail position on dose distribution for both IMRT and VMAT and found a loss of up to 83% of PTV coverage by the prescribed dose depending on whether the rails were positioned "in" or "out" and demonstrated that ignoring these couch components reduced the calculated tumor control probability (TCP) by about 8%. However, sparing of the critical structures (other than skin) changed little
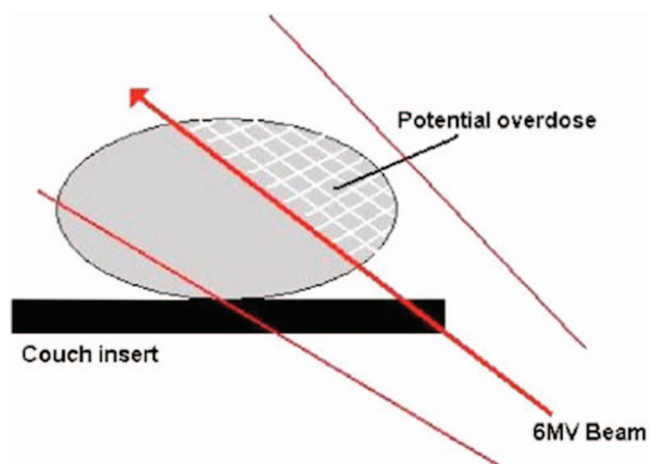

FIG. 5. Differential effect of dose perturbation for a 6 MV beam oblique to couch top partially passing through the couch top. From McCormack, Diffey, and Morgan, "The effect of gantry angle on megavoltage photon beam attenuation by a carbon fiber couch insert," Med. Phys. **32**, 483–487 (2005).
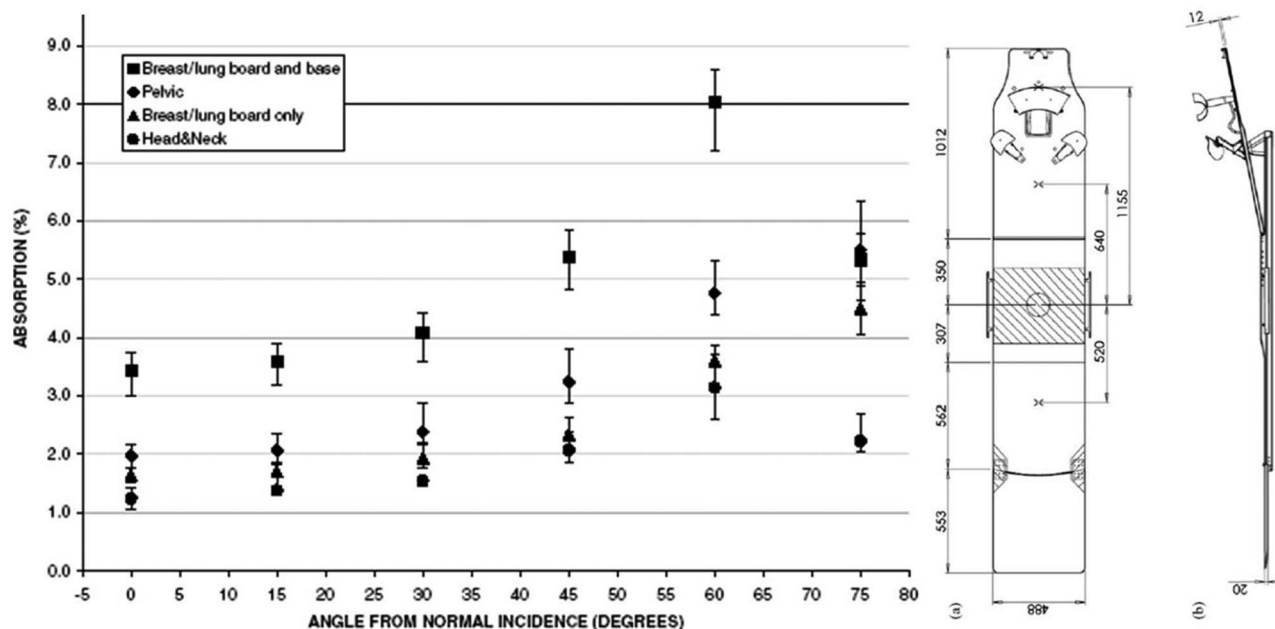
FIG. 6. Attenuation for the Contesse couchtop for 6 MV x-rays. From Berg *et al.*, "Absorption measurements on a new cone beam CT and IMRT compatible tabletop for use in external radiotherapy," Phys. Med. Biol. **54**, N319–N328 (2009).

with the presence or absence of the couch components in the plan. From the Pulliam paper, Figs. 7(a)–7(d) show 1, 2, and 3 Gy dose differences and Fig. 7(e) shows the DVHs with an IMRT or VMAT plan with the rails in or out. Pulliam's data also showed that the Varian mesh couch top alone introduced just a 4% PTV coverage loss for IMRT plans (compared to 20% loss for the imaging couch top) and an 8% loss with Rapid Arc plans (compared to a 43% loss with the imaging couch top).[9] Vanetti *et al.*[8] and Popple *et al.*[39] showed that the gamma agreement index for pretreatment QA had a larger variation across patients and an increased failure rate when the couch top was not included in the dose calculation.

2.B. Immobilization device effect on skin dose and attenuation

The accurate delivery of radiotherapy depends critically on the daily reproducibility of patient position. There is a wide range of patient immobilization equipment available to assist in positioning reproducibility. It has been reported that patient reproducibility can be as good as a few millimeters, which combined with IGRT can further reduce the interfraction positioning reproducibility to submillimeter level.[42, 43] However, as with treatment couch tops, the presence of immobilization devices in a radiation beam causes attenuation of dose at depth and an increase in skin dose. Even thin dressings placed on skin wounds can cause increased skin dose.[25] The sections below address common immobilization devices.

2.B.1. Body immobilization bags

Alpha-Cradles[TM] increase the skin dose even though attenuation may be small (approximately 1%).[7] Measurements show that both Alpha Cradles and vacuum immobilization bags (vac-bag) produce similar increases in the surface dose, raising it to about 68% from 16% for an open 6 MV beam.[44] Skin dose increases with the thickness and density of the formed bag. For vac-bags, the skin dose from a 6 MV 10×10 cm^2 field increased from 14% without the bag to 36% and 57% for a bag thicknesses of 2.5 and 10 cm, respectively.[45, 46] Ignoring the presence of a vac-bag and carbon fiber couch top, the planning system underestimated the skin dose by a factor of 2 for prostate patients treated with IMRT leading to grade 1 skin reactions in some patients. The WET for the vac bag was determined to be 0.2 to 0.5 cm.[47]

2.B.2. Head holders

The suitability of carbon fiber, PMMA and polystyrene foam for use in head holders was determined by measuring transmission and percentage depth dose in the buildup region for energies of 5, 6, and 8 MV. Carbon fiber was found to be less dose-perturbing than PMMA.[5, 48] Olch *et al.* reported the beam attenuation of the carbon fiber VBH HeadFix Arc (Medical Intelligence, Schwabmunchen, Germany) system to be 2%–4% in most sections, but was as much as 15% for the solid sections of the vertical posts.[49] Head and neck baseplates, typically made of 1 cm thick solid near-water equivalent material, should be fully encompassed in the planning CT field of view and included in the dose calculation for transiting beams.

2.B.3. Thermoplastic shells

Several groups have examined the effect of thermoplastic immobilization shells on surface dose for both photons and electrons and have concluded that they can significantly
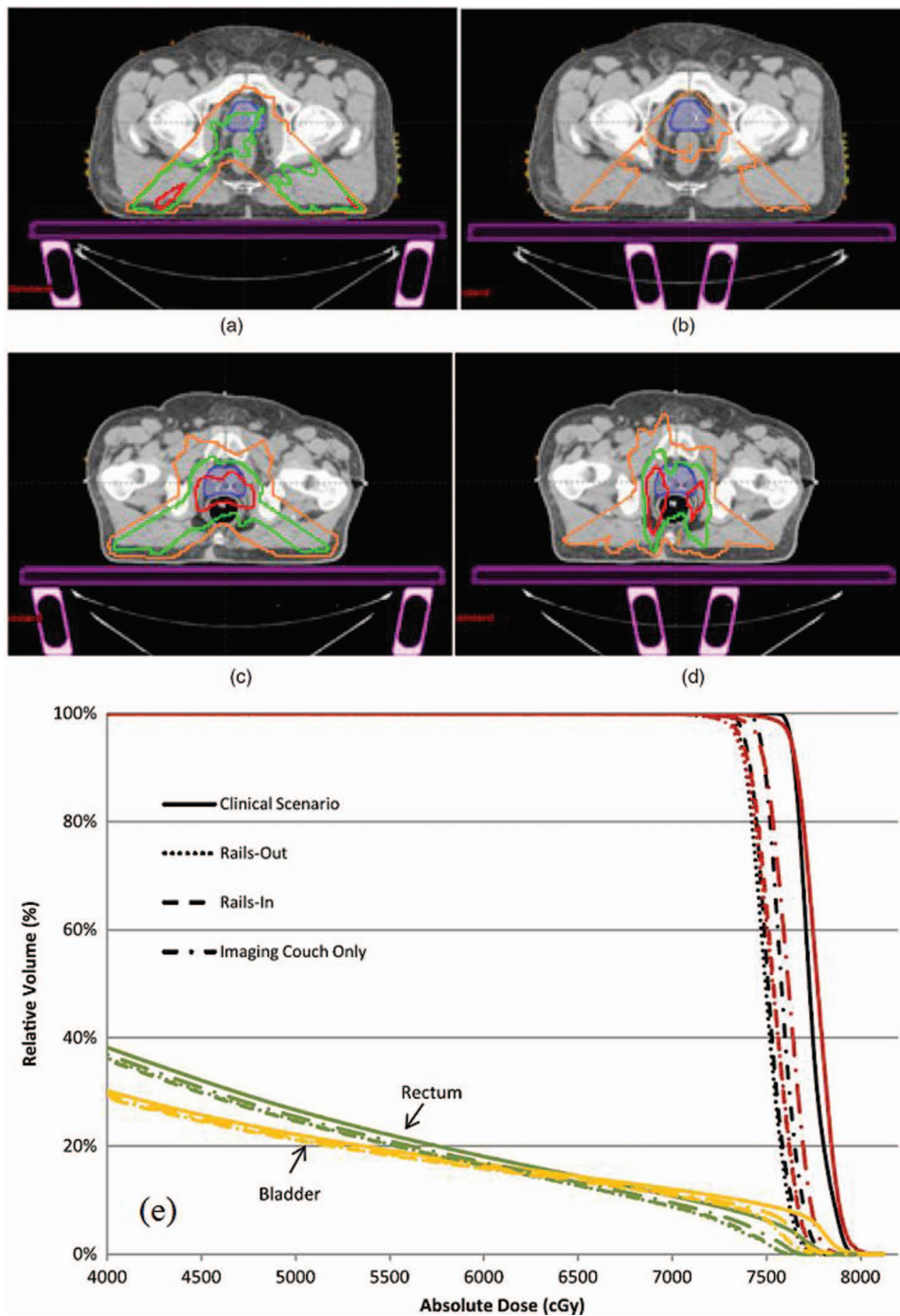
FIG. 7. Representative IMRT and RapidArc dose differences between the no-couch scenario and other plan iterations (a) IMRT rails-out, (b) IMRT rails-in, (c) RapidArc rails-out, and (d) RapidArc rails-in) showing spatially the areas of dose loss due to the couch and rails. Differences of 1, 2, and 3 Gy are shown. The outer-most line is 1 Gy, the next line interior is the 2 Gy line, and the innermost lines represent 3 Gy. The prostate/CTV is shown in solid colorwash. (e) DVH for RapidArc delivery to target and normal tissue structures for all plan iterations (no-couch, rails-out, rails-in, and imaging couch top only). The averaged PTV and CTV are shown as the outermost lines (black and red, respectively), along with the rectum (green) and bladder (yellow). From Pulliam *et al.*, "The clinical impact of the couch top and rails on IMRT and arc therapy," Phys. Med. Biol. **56**, 7435–7447 (2011).

increase skin dose.[29,31,50–54] Surface dose was found to decrease as the mask material was increasingly stretched which reduced the areal density and mask thickness (and reproducibility). For 6 MV photons, without stretching, the surface dose was 61% compared to 16% without a mask, but with stretching that increased the area of the mask by

125% or 525%, the surface dose changed to 48% or 29%, respectively.[50]

2.C. Equipment combinations

Immobilization devices are frequently connected to the couch top with a baseplate or similar device. These additional

devices, often made of carbon fiber, plastic, or aluminum, also increase attenuation and skin dose with a magnitude varying with type and composition of the device. The dosimetric effects of the combination of the couch top and immobilization devices are of course greater than either alone and it is the composite that must be considered in dose calculations. Skin sparing is greatly diminished by beam transit through the couch and the additional material of an immobilization device all but eliminates it.[55,56] Attenuation effects of up to 11% from the combination of couch and various immobilization devices including body and head frames used for stereotactic radiosurgery have been reported.[55,57–59] Many of the entries in Tables I and II relate to couch and immobilization device combinations.

2.D. Calypso

Calypso (Varian Medical Systems, Palo Alto, CA) is a 4D real time electromagnetic tracking system which monitors the position of an implanted transponder during radiation treatment. The patient lies on a Calypso overlay which replaces the couch top and an electromagnetic array is then positioned above the patient to facilitate transponder localization and tracking. No part of the system is present during CT treatment planning. For the Calypso array, Pouliot *et al.*[60] measured 0.5% attenuation in a prototype using normally incident 6 MV x-rays but others reported attenuation for the array in line with manufacturer's specifications, typically 1% to 2% at normal beam incidence, increasing with oblique beam incidence up to 5%.[61–63] Attenuation of the couch overlay was measured to be 1%.[63] Although not reported in the literature, for each patient, one could segment into the TPS a slab with accurate geometry and density so the dose calculation can account for this device.

2.E. Impact of external devices on clinical proton beams

When heavy charged particle treatment beams traverse the treatment couch or immobilization device prior to the patient, the distal range of the treatment beam is shifted toward the patient surface. Other effects such as changes in lateral spread and range straggling are usually minor with a couch thickness of about 1 cm WET. The change of proton distal range must be taken into account in the treatment planning process to accurately predict dose in the patient. The literature is sparse regarding the dosimetric effect of the treatment couch or immobilization devices for heavy charged particles.[64,65] For proton radiotherapy, the couch top and immobilization devices in the beam path act as range shifters, as shown in Fig. 8. If the treatment couch were not included in the dose calculation or not modeled correctly for a proton beam, a significant dose error would occur at the end of the proton range for the particular beam.

Carbon fiber couches with sandwich design are currently used in most of the proton centers in the U.S. The WET of the couch extension is used in dose calculations. The WET of a couch top can be determined experimentally (refer to Sec. 4
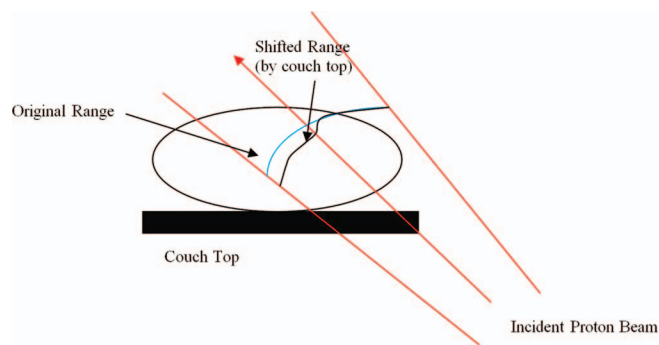
FIG. 8. Oblique proton beam incident on couch and shifted range.

for more details) or from a CT scan and used to determine the dosimetric impact of the device. For example, the WET of a Hitachi couch extension (Hitachi Ltd., Japan) was determined to be 1.1 cm, i.e., the couch would shift a normally incident proton beam by 1.1 cm toward the patient surface (Fig. 9). The actual path length in a patient plan depends on the beam incident angle and could vary significantly. Other couches currently used for proton therapy include the QFIX proton kVue couch (WFR Aquaplast, Avondale, PA) with WET of 0.55 cm and the QFIX Standard Couch with WET of 1 cm (WET values reported by private communication).

3. INCLUSION OF COUCH TOPS BY TREATMENT PLANNING SYSTEMS

3.A. Photon beam planning systems

Couch tops affect the dose distribution in a complex manner. This section will discuss the methods and accuracy of modeling carbon fiber-based couch tops by commercial TPSs.

Different TPSs handle structures external to the patient contour differently. Some completely ignore these structures while others do not if the density is above a certain threshold. In situations where portions of a device (or
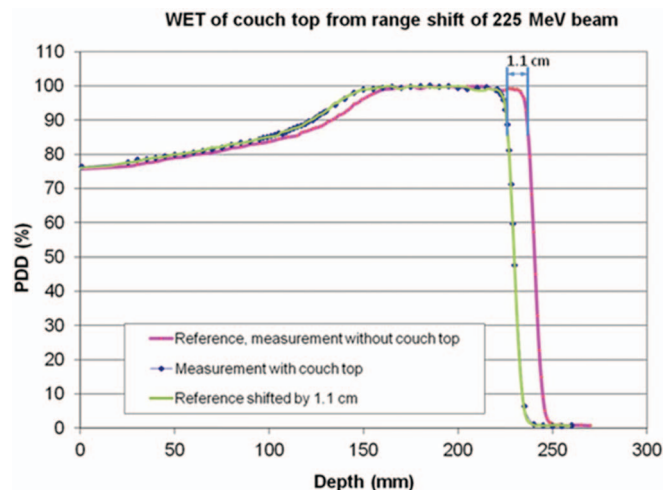
FIG. 9. PDD for protons with and without couch top (from unpublished MD Anderson commissioning data).
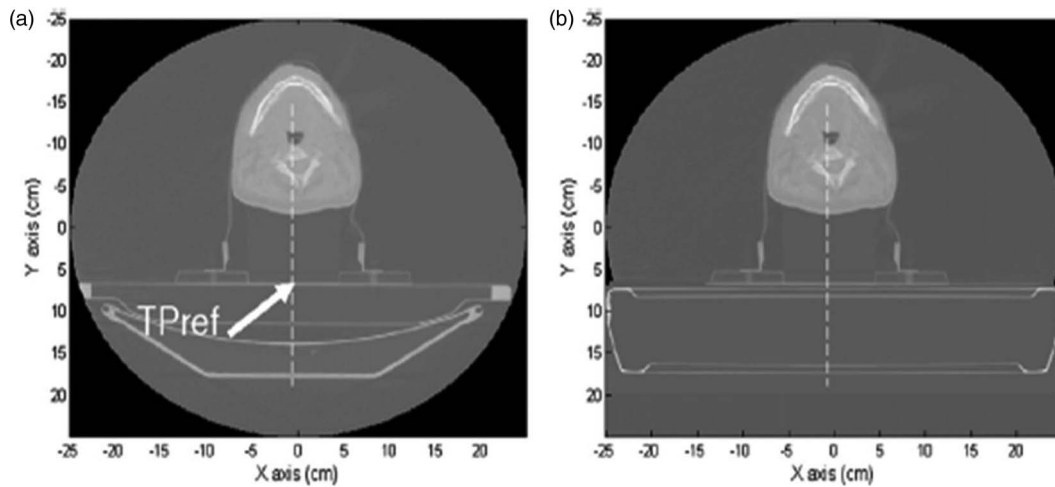
FIG. 10. Incorporation of a CT scan of carbon fiber treatment couch by modification of patient CT data sets. On the left a CT slice with the CT couch is presented, while on the right the same CT slice but with the treatment carbon fiber table is shown. From Spezi *et al.*, "Evaluating the influence of the Siemens IGRT carbon fibre tabletop in head and neck IMRT," Radiother. Oncol. **89**, 114–122 (2008).

anatomy) are excluded from the CT field of view, accurate calculations may not be possible without reintroducing the structures. Before attempting to segment into the planning CT the treatment planning couch top or immobilization device, one should first ascertain whether the TPS can accurately consider them by performing a simple test. Starting with a rectangular phantom, add a 2 cm thick slab 2 cm anterior to it (psuedo external device). The phantom can be designated as either "body" or some other structure type. An anteroposterior (AP) beam is applied with its isocenter at 5 cm depth in the "body" phantom. A dose calculation is performed and the dose at the isocenter found. A hand calculation is done which includes the slab. If these two dose calculations agree within about 1%, then the TPS is considering the slab. One should explore whether the TPS requires the structure type for the slab to be "body" or something else so that it is included in the calculation.

Two different approaches have been employed to include the couch top in the treatment planning process. The first integrates a CT scan of the treatment couch[11,13,37,41,66] into the plan, where the scanned treatment couch top is then inserted into the patient CT data set by TPS fusion modules,[41] third party software,[11] or in-house developed software. Couch modeling for a variety of commercial couch tops was performed in Theraplan (MDS Nordion, Uppsala, Sweden),[37] XiO (Elekta AB, Stockholm, Sweden), Oncentra Masterplan (Nucletron BV, Veenendal, the Netherlands),[13,66] and Pinnacle TPS (Philips Radiation Oncology Systems, Fitchburg, WI)[11,41] (Fig. 10). The pencil-beam type algorithms were usually unable to accurately estimate the couch attenuation at all gantry angles, confirming that modeling of electron transport is an important factor for comprehensive dose calculations. The results from dose calculations with the couch models included in the treatment planning process agreed with measurements to within 1.8% for 6 and 10 MV photon energies in situations where there was a 10% differ-

ence without the couch modeling.[66] In some cases, the TPS also accurately predicted the surface dose to within 3%.[13] When using a CT scan of the treatment couch top fused with each treatment planning scan, the same CT scanner for each should be used. Otherwise, the couch attenuation might not be correctly estimated due to differences in CT to density conversions between scanners. The inclusion of couch rails is more practical with the second approach described below.

The second approach utilizes automated[14] or manual[47] device contouring. The BrainLab (BrainLab, Heimstetten, Germany) IGRT couch top was modeled in the Pinnacle TPS through automatic contouring (realized by Pinnacle scripting) (Fig. 11) and the Sinmed carbon fiber couch (Siemens Medical Solutions, Concord, CA) in the Helax TMS (MDS Nordion, Uppsala, Sweden) TPS by manual contouring and assignment of appropriate WETs to the contours. This method was shown to perform similarly to the image fusion method described above.[47] A variation of this method is to create a drawing of the couch top in the planning system in a dummy patient image set and then create the DICOM RT Structure Set file containing this drawing. Each couch top in the clinic can be saved in a similar fashion in the same structure set file. This image set and structure set file can be registered to the actual patient image set at the time of planning and the saved couch structure can then be copied on to the patient's planning CT, effectively providing a library-based couch top insertion system.

TPS modeling of the couch top also allows the estimation of the bolus effect. Several researchers have shown that, at the radiological depth resulting from the presence of the couch top, effectively all of the TPSs are capable of accurate prediction of skin doses.[11,13,22,47,67] However, one must be careful to consider the volume averaging effects which can occur if there is an air gap between the couch top and the patient skin surface and the voxel assigned to the skin is partially in air
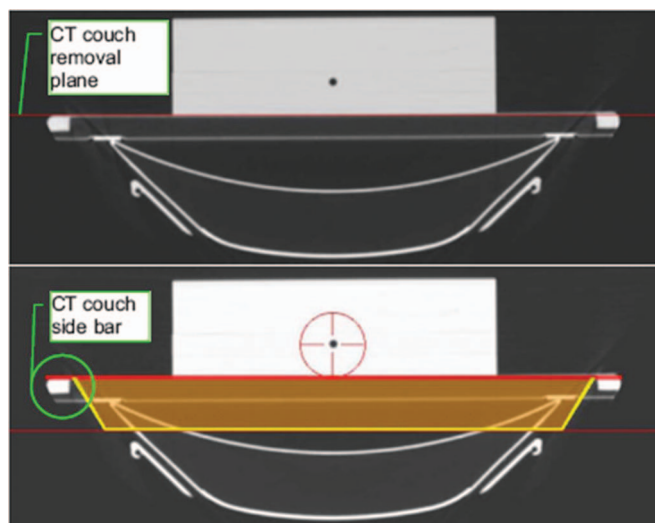
FIG. 11. Incorporation of a CT scan of carbon fiber treatment couch by couch contours. On the top a CT slice with the CT couch is presented, while on the bottom the same CT slice but with the contours of treatment carbon fiber table is shown. From Mihaylov *et al.*, "Modeling of carbon fiber couch attenuation properties with a commercial treatment planning system," Med. Phys. **35**, 4982–4988 (2008).

and partially in the patient. The dose value calculated for this voxel is based on the average density of the voxel. Reducing the CT image and calculation grid voxel size minimizes this effect. One must also carefully select the HU threshold that defines the skin surface.

Clinical implementation of TPS couch top modeling requires adequate commissioning and validation measurements of the device in the TPS. It should be noted that some couch tops have cross-sectional features which vary longitudinally while some are longitudinally uniform. TPS couch models must include all sections that can be in the treatment volume. Approximation of the actual couch geometry by solid slabs representing the WET of the treatment couch may produce inaccurate dose calculations depending on the beam geometry and is therefore not recommended. Moving the immobilization device longitudinally between CT simulation and treatment should be discouraged since different attenuation could result depending on the longitudinal symmetry of the couch top structure. Regardless of the method of TPS couch top insertion and features of the couch top, a rigorous method for reproducible patient indexing is required to preserve the patient-couch geometry between planning and delivery.[13,14] One can minimize or even eliminate the effort needed to model the couch by installing matching couch tops in the CT simulator and linear accelerator.

As of the end of 2012, automated couch insertion routines are available from Tomotherapy, Varian, and Brainlab. In the Tomotherapy Hi-Art (Accuray, Sunnyvale, CA) the coronal plane containing the top surface of the CT couch is identified in the patient image set. On each slice of the patient CT dataset the part of the image below this coronal plane is replaced with a CT image of the Tomotherapy Hi-Art unit couch which is positioned in the correct place relative to the patient.

This treatment couch replacement has appropriate predefined densities.

The Varian Eclipse TPS includes models of the Varian IGRT, Brainlab, and Exact couch tops (derived from technical drawings) for automatic inclusion into a plan. The couch top structure includes as separate entities, the rails, the couch shell, and the interior of the couch top. The CT number for each of these components can be assigned. During commissioning, the medical physicist should verify the accuracy of these structures in the TPS by comparing measurements to dose calculations and adjusting the CT number assignments to optimize the agreement.[8,9,39] The position of the rails of the Exact couch, either in or out, can be selected and the position of the entire couch top can be adjusted to the correct location relative to the patient. Users must apply quality assurance measures daily which enforce the planned couch and rail positions. Vanetti *et al.* concluded that Eclipse modeled the couch attenuation to within 1% based on optimized Hounsfield Unit (HU) numbers for the outer couch shell and the internal foam filling, thus correcting up to 4% dose errors found without inclusion of the couch top.[8] Wagner and Vorwerk also recommended use of different HU values than the Varian default values but Pulliam's results showed that the Varian default values were accurate.[68] Results of Monte Carlo modeling of the Varian couch top for use with RapidArc treatments suggested similar HU assignments as Vanetti *et al.*[10]

BrainLab (BrainLab, Heimstetten, Germany) iPlan TPS (RTDose 4.x) also allows a user to add a couch top model to the patient CT data set similar to the system in Eclipse. Furthermore, it is possible that users can create couch models, based on geometrical information of the individual composites (derived from technical drawings) and material properties (i.e., electron densities). Verification of the couch top model is performed by the user through comparison with CT scans of the actual treatment couch top. However, CT scans of the couch tops are not always possible and therefore an alternative method for verification would be to investigate and document the couch top radiographically and/or dosimetrically as described in Sec. 6 of this report.

Elekta (Elekta AB, Stockholm, Sweden) currently supports automatic incorporation of patient support devices in Monaco 3.1.0. The user can contour their own couches and immobilization devices to include them in a library for planning. The couches can be placed in the library as stand-alone devices. The user is responsible for assigning the appropriate density to the sample couches and fine tuning these values based on measured data. In XiO, a couch structure can be incorporated in the planning process if the device is scanned together with the patient or the user supplies external contours representing the device. The contours have to be either part of the patient or part of the external contour. Each contour can be assigned a specific density, thereby properly accounting for couch attenuation effects.

Couch top implementation in Pinnacle TPS is currently under development. Couch tops will be incorporated into the treatment planning process by contours derived from technical drawings as well as CT imaging studies of the

devices. The physical densities of the couch top components will be based on couch top technical specifications and will be fine-tuned based on absolute dosimetric measurements as well as CT imaging data where available. Until then, the scripting utility can be used to incorporate couch tops into Pinnacle.

3.B. Proton beam planning systems

Presently, several vendors offer proton treatment planning systems; Elekta (XiO), Varian (Eclipse), RaySearch (Ray-Search Laboratories AB, Stockholm, Sweden) (Raystation) and Philips (Pinnacle) (under development). Those TPSs are based on pencil beam algorithms although Monte Carlo systems are under development. Using artificial tissue phantoms, a CT number-to-density calibration is established and the CT numbers are converted to relative proton stopping powers and then to WET for dose calculations.[69] Since the material composition and thus relative stopping power of the treatment couch top and other patient supporting devices are usually different from the artificial tissue materials used in the CT number calibration process, potential errors could be made in the stopping power calculation if the tissue phantom calibration were used. Instead, one must independently know the proton stopping power for the various materials used in the couch top.[70] To address this in the TPS, one commonly used technique is to use a scan of the treatment couch top which then replaces the CT couch top in the planning CT and assign CT numbers to the couch top structures which will cause the dose calculation to use the known proton stopping power. The calculation should be validated with measurement during the commissioning of the TPS/supporting device (see Sec. 4). None of the commercially available TPSs currently support automatic inclusion of a couch top. For beams that pass through the treatment couch top and/or patient immobilization devices, especially the nonuniform regions such as edges of the couch top, it is highly recommended to take into account the uncertainty of device WET due to CT number calibration and patient setup, when designing beam specific margins and compensator smearing.[71,72] This practice could minimize the dosimetric impact of such uncertainties on the target coverage.[65] Rounded edges of the couch top are preferred to minimize these effects. Using the same couch top for planning as for treatment simplifies some of these procedures.

Some of the proton beam planning systems require an external contour for dose calculation. Material outside of the external contour is ignored and dose is not calculated in these areas. Users of such systems should also verify that the external contour encompasses all patient support devices used for treatment.

4. MEASUREMENT METHODS FOR ATTENUATION AND SURFACE DOSE FROM EXTERNAL DEVICES

This section outlines the measurements that should be made to characterize attenuation and surface dose perturba-

tions caused by devices external to the patient and provides an overview of the various detectors suitable for performing these measurements. It also includes recommendations for data and documentation that should be provided by manufacturers of such devices. Ideally, all treatment devices and patient support systems intersected by the treatment beam should be included in the TPS calculation model. The data obtained from the measurements outlined in this section will be useful for the validation of the TPS. In addition, the data set described here could be used to estimate correction factors (if the TPS is not used), to identify geometries that should be avoided clinically, or to validate independent calculation methods.

4.A. Methods of attenuation measurements

4.A.1. Geometry for attenuation measurements

The large number of geometric relationships among the beam source (gantry angle, collimator angle, field size) and the beam perturbing device makes it impossible to perform measurements representative of all clinical situations. Therefore, it is important to acquire data representative of typical as well as worst case clinical conditions for beam perturbations. Measurements should at least include the most probable treatment geometries (e.g., IEC gantry angles of $120°$ and $180°$ for perturbation effects of patient support devices) as well as those geometries that represent the worst case scenarios such as maximum attenuation or geometries resulting in large attenuation gradients such as those that can be expected near the edge of a support device. These measurements characterize the attenuating properties of the device and should be used to validate TPS calculations that include them. Determining the worst case geometry may most easily be achieved by taking a CT scan of the device in question and looking for paths of greatest integrated mass. Alternatively one could use manufacturer supplied drawings or use the linac Electronic Portal Imaging Device (EPID) to search for the region of greatest attenuation. Many treatment support devices do not have homogenous construction, and care should be taken to examine the full longitudinal and lateral extent of the device that can be intersected with the beam during treatment. Measurements made near d_{max} will be insensitive to attenuation by a 5 to 8 mm WET for 6 to 18 MV x-rays due to the broad shoulder of the depth dose curve. Depths much greater than d_{max} (we recommend 10 cm) should be used for attenuation measurements.

A common geometry used to measure attenuation by patient support devices[13,21,37,41] is shown in Fig. 12. A 20 cm diameter cylinder with an ion chamber at its geometric center is positioned such that the ion chamber is at the linac isocenter. This can be verified by physical front pointer measurements for $0°$, $90°$, and $270°$ (IEC gantry angles) or by ionization measurements; in either case, the same value should be obtained at all angles. Also the center of the phantom must be at the lateral center of the couch. This can be verified by ensuring that the sagittal laser passes through the center of the couch and the phantom. In the section that
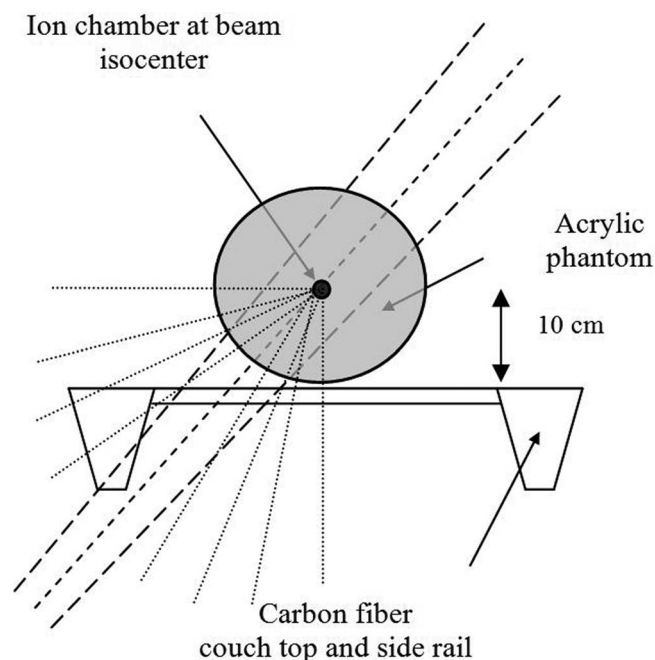
FIG. 12. 20 cm diameter cylindrical phantom centered on couch with ion chamber at center, beams every 10° from 270° to 180°. Adapted from Gerig *et al.*, "Dose perturbations by two carbon fiber treatment couches and the ability of a commercial treatment planning system to predict these effects," Med. Phys. **37**, 322–328 (2010).

follows, we have recommended that manufacturers of patient support devices provide attenuation maps for this geometry and hence for comparative and standardization purposes the user should make attenuation measurements under the same conditions. Note that this geometry does not measure attenuation directly; rather it measures the dose perturbation at depth in a phantom resulting from beam attenuation external to the phantom.

If a cylindrical phantom is not available, then the user may make measurements in a rectangular phantom (i.e., 30×30 cm^2 slabs stacked 20 cm deep) at 180° (and 0° as its reference) but other angles will be error prone due to the need to account for the path length differences through the phantom at the various gantry angles. The ion chamber, couch, and phantom geometry should be the same as for the cylindrical phantom method mentioned above and in Sec. 4.C. Instead of relying on a single unattenuated field reference measurement as can be done with a cylindrical phantom, each angular measurement for beams passing through the couch top and rectangular phantom must be accompanied by a reference measurement provided by a 180° opposing beam (which does not pass through the couch top). The accuracy of the opposing gantry angle should be 0.5° to maintain less than 1% error due to differences in path length through the phantom of the reference beam and the couch top measurement beam. The user should account for differences in output vs gantry angle for these angular measurements. At a minimum the user should make measurements at gantry angles between 110° (or whatever angle causes the central axis to penetrate the couch top) and 180° in 10° increments for the 10×10

cm^2 field. Smaller or larger fields can also be used and will be useful in characterizing TPS accuracy. To determine the attenuation for a beam perpendicular to lateral sections (i.e., rails) of the couch top requires the phantom to be translated to those locations and then 0° and 180° gantry angle field measurements made. These measurements might be useful as supplements to those using oblique beams for TPS dose verification.

4.A.2. Methods of attenuation measurement

4.A.2.a. Point measurements. Cylindrical ion chambers are the most commonly used dosimeter for single point measurements of attenuation by objects such as the patient support or immobilization devices. At depths greater than the depth of maximum dose, in-phantom measurement of dose reduction caused by external devices does not present the same challenge as the measurement of surface dose. The dose reduction caused by an external object at the point of interest is the ratio of the dose with the attenuating object in place to the dose with the attenuating object absent. It is safe to assume that under the conditions defined above, the ratio of dose is equal to the ratio of ionization. Care should be taken that the chamber properties such as cavity dimension are appropriate for the measurement conditions. The WET can be determined from attenuation measurements by noting the depth increment in the applicable tissue maximum ratio (TMR) table (at 10 cm depth) needed to reduce the dose by the amount of the measured attenuation.

4.A.2.b. 2D measurements. Two-dimensional measurement of attenuation has important advantages over single point measurement, making it easier to identify regions of greatest attenuation and regions of high dose (attenuation) gradient. The most common 2D measurement is either by film or by EPID. Film (either radiographic or radiochromic) can measure either in-phantom dose or exit dose, while in general the EPID can only perform transit dosimetry. In many cases, exit dosimetry can be used to compare the dose to a given location in the image where the beam passes through the external structure to the dose to a nearby location without the external structure. Accurate determination of attenuation using exit beam images is much more complicated than ion chamber measurements of attenuation. Over the past few years the use of EPID has eclipsed the use of film in routine clinical practice. Vieira demonstrated that EPID images can be used to detect whether the rail or couch top frame was inadvertently in the beam as well as to quantify the attenuation of each part[73] (Fig. 13). More recently, Ali *et al.* demonstrated that the treatment couch attenuation could be included in the portal image dose prediction.[74] The ability to back-project exit images to the patient in order to calculate dose (or attenuation) has greatly improved,[75] but while accurate dosimetry with an EPID is possible, it is complicated.[76] For example, EPIDs have been shown to have variations in pixel sensitivity[77] and a strong spectral response[78] as well as significant field size dependence.[79] In a literature review van Elmpt *et al.* provide an excellent review of EPID based dosimetry.[80]
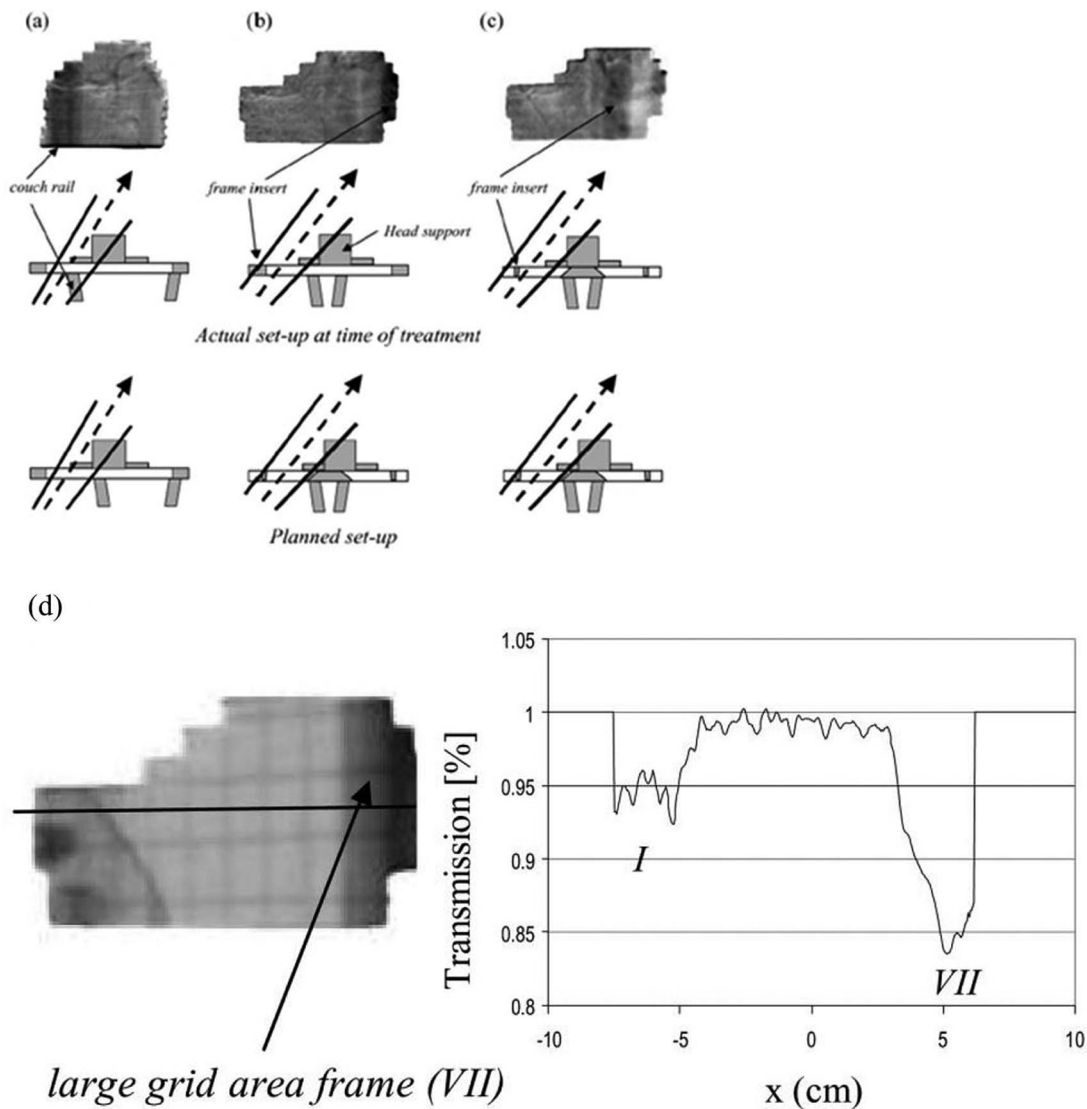
FIG. 13. EPID images demonstrating setup errors relative to couch rails (a–c). Measurement of beam attenuation by couch and couch rails (d). From Vieira *et al.*,"Two-dimensional measurement of photon beam attenuation by the treatment couch and immobilization devices using an electronic portal imaging device," Med. Phys. **30**, 2981–2987 (2003).

4.B. Surface dose and buildup measurements

4.B.1. Geometry for surface dose and buildup measurements

Surface dose and the rate of dose build up have long been known to be dependent on energy, field size, and beam geometry.[81] In the case of megavoltage photon beams, the surface (skin) dose arises from backscatter within the patient and from photon interactions creating secondary electrons which occur upstream in the air and in solid materials such as the collimators, blocking trays, flattening filters, and support devices and is dependent upon geometric factors such as distance, field size, and beam obliquity.[82]

Measured data can be used to validate TPS calculations or can be used directly to estimate patient skin dose under specific clinical conditions. Although full buildup curves over a range of beam incident angles are desirable, a minimum set of measured data should include the surface dose and depth of maximum dose for normally incident beams over a range of field sizes and beam energies that cover all clinical applications. These will act as a reference for clinical devices that alter skin dose and can be used as input or test data when commissioning a TPS.

Couch tops and other devices in direct contact with the patient can be treated dosimetrically as part of the patient. With this approach the user can measure the attenuation through various parts of the couch at appropriate beam angles and determine the WET for the given geometry. In this case, knowledge of a device's WET combined with open field buildup PDDs can be used to estimate patient skin dose and depth of maximum dose for a given clinical situation. The user may also wish to compare the measured WET values with those supplied by the manufacturer—see recommended manufacturer supplied data requirements below. For reference, in

Tables III–V, we provide typical open beam percent depth doses for the buildup region for 6, 10, and 18 MV photon beams. These data were measured with an Attix parallel plate chamber which gives results similar to an extrapolation chamber.[83] In addition, Monte Carlo calculations of buildup percent depth dose support the values in the tables.[84] Note that these data are not for clinical use but can be used by vendors to standardize their reporting of surface dose from external devices. The actual buildup curves for a specific linac beam can differ from the data provided herein. As an example of how to use WET values combined with open beam buildup depth dose data, consider a couch top with a known WET of 4 mm for a normally incident beam. The estimated surface dose from a 6 MV 10×10 cm^2 posterior beam is 77%, found by looking at the buildup PDD at a depth of 4 mm in Table V. Directly measured surface dose can be accurately obtained within 10% of the local dose (1%–3% absolute) which corresponds to about 0.1–0.2 mm distance to agreement but accuracy within 5% absolute often provides a clinically useful result. The error in estimating inferred surface dose from typical external device WETs of at least 0.3 cm should also be less than 10% of the local dose.

4.B.2. Detectors used for measurement of surface dose and buildup

Although a measured WET combined with *a priori* knowledge of the open field buildup curve can be used to infer the surface dose, it is important to understand how surface dose can be directly measured. *In vivo* measurements for patient-specific skin dose determinations are often required when there is a suspicion that skin dose may be excessive. Treatments with a single PA beam, AP/PA beams, or plans with many beams for which the target volume is close to the skin can create this condition. Determination of surface dose by measurement is difficult and the choice of detector is critical. The typical setup for measurement of surface dose with a parallel plate ion chamber is to irradiate the chamber in a solid water phantom with no additional material between the collecting volume and the source. To assess the impact on surface dose of a device, such as the couch top, one would irradiate through the couch top with a PA beam with the chamber and phantom inverted so the chamber is lying on the couch top. Large dose gradients and electronic disequilibrium near the surface require the dosimeter to have a small, well defined measurement volume and to be insensitive to changes in the electron energy spectrum.[85] When choosing a detector for a specific measurement, characteristics such as spatial resolution, dose range, accuracy, precision, angular dependence, spectral (energy) dependence, and the effective depth of measurement must be considered.[13,86–89]

In general it is assumed that for ion chamber measurement in photon beams at depths greater than d_{max}, the perturbation correction factors and the stopping power ratios are independent of depth and the ionization ratio can be considered equal to the dose ratio.[84] In the buildup region or other regions where electronic equilibrium does not exist, this assumption is not necessarily valid. The design and geometry of the ionization chamber influences the perturbation factors required to calculate unperturbed ionization. Fluence perturbations usually result in an over response of the detector and an over estimate of the PDD if not properly addressed.[90] The magnitude of the error is detector and beam specific. The user should take care to understand the magnitude of error and uncertainty for their given experimental conditions.

The most common detectors used for the measurement of buildup and surface dose are extrapolation chambers, plane parallel chambers, TLD, and film. Cylindrical ion chambers are not recommended for megavoltage surface dose measurements due to the large chamber-dependent corrections needed to get an accurate dose. There are also numerous reports in the literature describing the use of diamond, diode, optically stimulated luminescent (OSL) detectors, and metal oxide semiconductor field effect transistor (MOSFET) detectors. Below we provide specific information about each type of detector.

4.B.2.a. Extrapolation chamber. The extrapolation chamber, designed by Failla in 1937,[91] is still accepted as the "gold standard" for surface dose measurement of MV beams, primarily because most perturbations introduced by ion chambers are eliminated with the use of an extrapolation chamber.[92,93] It is often implied or suggested that the extrapolated zero volume ionization ratio (PDI) gives the PDD.[87,90,94] In fact the extrapolated zero volume ionization gives the true ionization that would have occurred if there were no perturbation effects. The change in stopping power ratio from the surface to depth of maximum dose still remains a source of uncertainty in converting PDI to PDD even with an extrapolation chamber. Although considered the gold standard, their use is very time consuming, costly, and not practical for multi-field measurements causing many physicists to use other detectors.

4.B.2.b. Plane parallel ion chambers. Plane parallel ion chambers are a viable alternative to extrapolation chambers, but unlike extrapolation chambers, perturbation corrections are required under disequilibrium conditions. This was addressed in detail by Velkley *et al.* who used extrapolation chamber data to develop an empirical correction (k_{ion}).[93] The approach was later refined by Gerbi and Khan[87] to account for the guard ring dimensions of the fixed parallel plate chamber. Failure to account for perturbation can result in an up to 15% (absolute) over-response in the determination of surface dose.[87]

In general, parallel plate ion chambers display a polarity effect, which can be significant in regions of electronic disequilibrium such as the dose buildup region. This has been documented as early as 1951 by Howarth *et al.*[95] and studied in detail by Gerbi and Khan.[87] The present day consensus is that for measurements using parallel plate chambers the average of the dosimetric signal measured with positive and negative bias should be used to estimate ionization. For parallel plate chambers, beam geometry is important. As shown by Gerbi and Khan[87] and by Dogan and Glasgow,[86,88] the perturbation caused by in-scattering increases with obliquity of the

incident photon beam. A table of the common parallel plate (PP) chambers and their respective physical characteristics is given in the Appendix.

4.B.2.c. TLD. TLD, most commonly LiF, is frequently used for the estimation of *in vivo* skin dose and for the measurement of dose buildup curves. TLDs come in various forms, such as rods, chips, wafers and powder. The thickness of the standard TLD chips presents a problem for the direct measurement of surface dose, as they have been shown to overestimate the dose by a factor of about 2.[90] Several approaches have been developed to circumvent this problem. Kron *et al.* used three different thicknesses of TLD to extrapolate to the surface dose and reported good agreement with parallel plate ion chamber measurements. They demonstrated that the TLD response is not linearly dependent on the depth of the TLD geometric center, and a linear fit leads to overestimation of the surface dose.[96,97] A similar extrapolation method was developed based on TLD powder.[98] Thomas *et al.* doped TLDs with carbon, which prevented light arising at depth in the TLD from escaping so that although their TLD was 0.4 mm thick, the effective point of measurement was <0.07 mm.[99]

TLDs have some advantages over parallel plate chambers for the measurement of surface dose for obliquely incident beams[87] and multiple fields. Stathakis *et al.* using ultra-thin (0.1 mm) TLD, demonstrated good agreement with Monte Carlo calculations over a range of beam angles and energies. They report overall uncertainties of 3% to 5% which can be reduced to 1% to 3% if the TLDs are calibrated for each photon beam.[88] Similarly Nilsson *et al.* have shown that thin TLDs with a thickness of 0.13 mm are suitable for skin dose estimation and accurate to within 5% (absolute) if appropriate correction factors are applied.[90]

4.B.2.d. Film. Film is a good alternative to point dosimeters such as TLD and ion chambers. It provides the advantage of measuring dose in a plane or surface from an entire field in a single measurement with extremely high spatial resolution. The use of film to measure dose build up and depth dose has been described as early as 1951 by Greening.[100] There are two basic types of film used for radiation dosimetry; radiographic film, and radiochromic film, and there are multiple versions of each.

Conventional film has been used by many investigators to examine surface dose as well as dose distribution, although some investigators suggest that silver halide film is less suitable for surface-dose measurements than radiochromic film due to significant over-response to low-energy radiation by the silver (e.g., 1000% below 80 keV).[101] The AAPM Task Group 69 report provides recommendations on using standard radiographic film and discusses limitations and uses.[102] They suggest that using "ready pack" film will give a surface dose about 10% (absolute) above the dose determined by an extrapolation chamber, an offset which one could use as a correction factor. Butson *et al.* describes an extrapolation technique using a series of radiographic film layers to produce an extrapolated result and showed that the percentage surface dose can be estimated within ±3% of parallel plate ionization chamber results.[103]

Radiochromic film differs from radiographic film in that the image is formed directly as a result of energy absorption and does not require chemical processing to reveal the image. Niroomand-Rad *et al.* provided an excellent primer on the history, use and physical basis of radiochromic film in the report of AAPM Task Group 55.[104] There are many different types of radiochromic film with a variety of properties, and much of the film described in early reports is no longer commercially available. Therefore, AAPM Task Group 235 of the Therapy Physics Committee was formed to update the AAPM TG 55 report. Defining and correcting for the effective point of measurement is an issue with both radiographic and radiochromic film. Devic *et al.* used the high sensitivity radiochromic film models HS, EBT, and XR-T, to obtain the skin dose at a depth of 0.07 mm. They demonstrated that skin dose corrections for the effective point of measurement are negligible for the radiochromic film models used.[85] Other investigators used extrapolation methods employing film stacks to determine surface dose and generally reported agreement to within 2%–3% of extrapolation and PP chamber results.[105,106] The effective point of measurement should be determined for each type of film model and batch number when used for these measurements.

4.B.2.e. Diamond, MOSFET, OSL, and diode detectors. Diamond detectors act as solid state ionization chambers that, unlike most diodes, are insensitive to radiation damage.[107] Although not in common use, they have very good spatial response, are nearly tissue equivalent and behave like PP chambers in the buildup region.[108] De Angelis *et al.* have reported significant variation in the properties of diamond detectors of the same model, which then requires that the users characterize each detector prior to use. Properties that should be characterized include: time stability, response variation with accumulated dose, angular dependence, preirradiation conditioning dose, temperature coefficient, dose rate dependence, polarization effects, response time, and signal stability.[109,110] Although diamond detectors can perform as well as ion chambers and are especially useful for small fields or when tissue equivalence is needed, given the drawbacks mentioned above and high cost, they are not commonly used.[110] Scherf intercompared the surface dose from a nonenergy compensated diode and a diamond detector and found a 6%–9% difference, increasing with field size, for a 6 MV beam and about 3% for 25 MV irrespective of field size.[111] A noncommercial MOSFET was used for surface dose measurements compared to TLD and an Attix parallel plate chamber. Photons (6 and 18 MV) and a range of electrons were measured and the MOSFET doses were in agreement (within 3%) with the other detectors.[112] Others have made skin dose measurements with MOSFETS and diodes for multibeam treatments and have found each to be useful.[54,113] OSL detectors have also been used for skin dose measurements and have been found to be sufficiently accurate.[113,114]

4.C. Manufacturer supplied data (photons)

For the purpose of standardization of measurement methodology, comparison across devices, and to aid

verification of TPS modeling, we recommend that manufacturers of patient support devices provide the following data:

i. A polar distribution of attenuation and WET in the area of the device most likely to be irradiated during treatment as well as any areas of the couch top designated for a specific purpose (e.g., a specialized head and neck section). The geometry shown in Fig. 12 should be used. Here a 20 cm diameter cylinder with an ion chamber at its geometric center is centered on the treatment couch and is positioned so that the ion chamber is at linac isocenter. Measurements should be made every 10° from normal incidence through the couch top to the largest angle for which the central axis of the beam traverses the couch top and any other permanently attached immobilization device. The dose for a 90° (lateral) beam will be measured and will serve as the normalization for the other angles. Attenuation at each angle should be provided for nominal beam energies of 6, 10, and 18 MV for a 10×10 cm^2 field size. The manufacturer should specify the PDD$_{10}$ or TPR$_{20/10}$ for each beam used. The WET will be computed by referring to the appropriate TMR table and finding the incremental depth beyond 10 cm that would result in the attenuation measured at the nominal depth in the phantom.

ii. Attenuation and WET for a beam normal to the most attenuating parts of the device (which have not been labeled as regions to avoid) should be documented by the location and percentage attenuation and WET.

iii. Surface dose for the angular and energy range in item i., computed by using the PDD values in Tables III–V and recording the surface PDD for a depth equal to the WET. This measure of surface dose is a calculated value and not necessarily the dose one would directly measure at the surface of the phantom.

4.D. Proton beam measurements

4.D.1. Measurement methods

As discussed in Secs. 2 and 3, patient support devices in the proton beam line act effectively as a range shifter, and measurements should be used to validate the WET of the device calculated by the TPS, as well as the surface dose change. A CT scan of the couch top is necessary to identify any nonuniformities in the couch top, and the TPS should be used to calculate the WET of the couch top using the CT number-to-stopping power calibration. Supporting devices should always be in the field-of-view (FOV) for the patient CT scan. The TPS calculated WET should be compared with measurement, manufacturer supplied data and independent calculation during the commissioning of the TPS to ensure that the couch was modeled properly.

For proton range measurements, it is critical to accurately determine the depth of measurement for all measurement points. Proton PDD and range measurements have traditionally been made with a water-scanning parallel plate chamber. This process is time consuming as scanning with submillimeter step sizes are required to resolve the Bragg-peak or the distal end of a spread-out-Bragg-peak (SOBP). With the introduction of a multi-layer ion chamber device (e.g., Zebra, IBA Dosimetry GmbH., Schwarzenbruck, Germany) which can scan an entire proton PDD curve almost instantly, measurements of proton range and PDD are becoming more efficient. Two-dimensional range and profile measurements can be made with films or detector arrays such as Matrixx (IBA Dosimetry GmbH. Schwarzenbruck, Germany). For WET measurement, the same setup as the proton range measurement can be used. Range measurements with and without the patient supporting device in the beamline should be made with the range difference between the two measurements being the WET of the device. Parallel plate chambers or TLD can be used for surface dose measurements in proton beams without the electron equilibrium considerations for photon beams as the PDD is nearly flat for a depth much greater than the dimensions of most detectors used for beam scanning or point dose measurements.

The PDD with and without the Hitachi treatment couch top were measured with an Advanced Markus (PTW, Freiburg, Germany) parallel plate ion chamber, for a proton beam with energy of 225 MeV, SOBP of 10 cm, and range of 23.6 cm. The measurement was made in a water tank for depths between 2 and 27 cm, and an additional in-air measurement was made for the surface dose. The range of the proton beam was determined from the PDD with and without the couch top in the beam, and range change due to the couch top was found to be 1.1 cm (Fig. 9). This shift is applicable across all depths measured. The surface dose change was determined to be <1%. The beam was normal to the couch top for these measurements. Couch top induced range effects at oblique angles are difficult to measure and generally have to be inferred from the TPS calculations that have been validated at normal beam incidence. For patient supporting devices, the WET of the device at different locations should be measured, with the same technique discussed above. The measurement results should be compared with the WET as calculated by the TPS at the same locations. If a discrepancy between measurement and the TPS calculation of greater than 2 mm is found, the material of the device and the CT calibration curve should be verified. To account for this discrepancy, techniques such as CT number overwriting (Sec. 3.B) or using additional margins in the planning process for beams that transverse the device can be used.

4.D.2. Manufacturer supplied data (protons)

We recommend that manufacturers of couch tops and other patient support devices for proton radiotherapy provide the following data:

1. Material composition of the device, and relative stopping power ratio of individual materials.
2. WET for a 200 MeV proton beam incident normal to and at the center of the device surface.

3. WET and its location for a 200 MeV proton beam incident normal to the device surface at the point of greatest WET.

5. AVOIDANCE OF EXTERNAL DEVICES DURING TREATMENT PLANNING

Although using one's TPS to calculate the dose including the presence of couch and immobilization devices is optimal, not everyone has this ability. This section describes the next best approach, which is to visualize the devices in the TPS using beams-eye-view (BEV) methods to avoid beams passing through the dose perturbing structures. In the worst case, where the couch structures are absent from the planning CT, one can still use methods to estimate their locations so that beams can be planned to avoid passage through them. When applying these methods, one should allow for uncertainties in the exact location of the external devices relative to the patient introduced by patient position verification couch shifts.

5.A. Couch top avoidance

The need for a simple method to determine if a beam will pass through part of the couch top has been addressed by using analytical methods with acceptable accuracy.[115] Gantry, couch, and collimator angle, as well as jaw and MLC positions were all considered in a geometrical model used to calculate beam ray intersections with the couch top.[116] More recently, software methods using a graphical user interface separate from the TPS have been developed.[117]

As IMRT became more widely used with larger numbers of equally spaced coplanar beams, it became apparent that intersections with absorbing parts of the couch were common unless this was detected in advance and alterations to the treatment plan were made. In one study, either frame positions (i.e., rails) were moved or gantry angles were changed to avoid the intersection. Beam intersections occurred in 63% of the plans, requiring a gantry rotation of one or more beams. They concluded that dose distributions for a prostate treatment would not be affected detrimentally by rotating two posterior-oblique beams by 10° to avoid the intersection.[118]

One can estimate whether posterior oblique beams will intersect the couch frame or rails using generally available TPS ruler tools. Figure 14(a) shows the Eclipse TPS insertion of an Exact couch top under the patient CT for an 8 beam coplanar IMRT plan. There are two posterior oblique beams which potentially intersect the rails. The right edge of the right posterior oblique beam (RPO) is extended by using the ruler tool to show that it just skims the inside corner of the right side rail or a beams-eye-view can be used. When an automatic couch top inclusion feature is not available in the TPS, then one can manually determine the extents of the couch rails as shown in Fig. 14(b). Here one must measure the width, height, and distance from the couch midline to the couch rails and use ruler tools, to map out the location of the inner edge of the rail. The right edge of the RPO beam is extended toward the
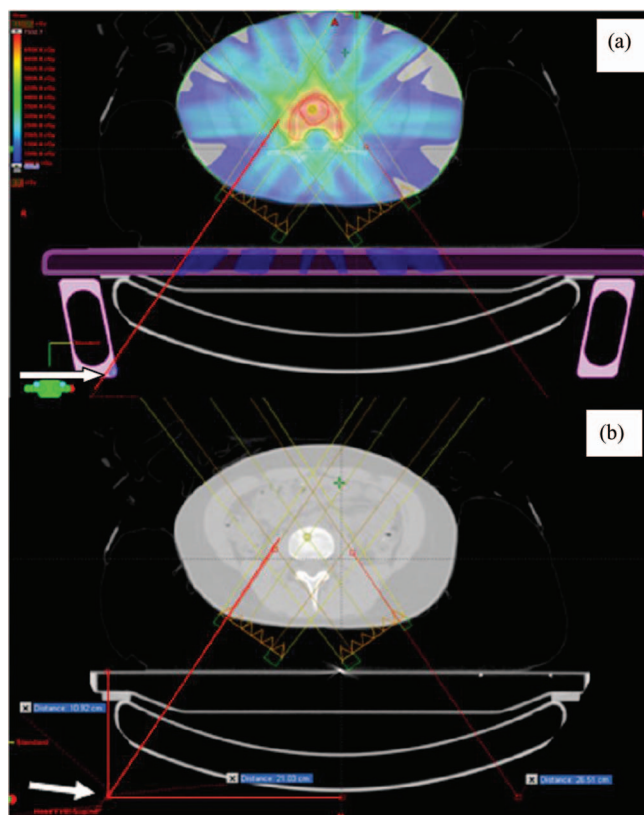

FIG. 14. (a) Couch is modeled in TPS, manual extension of RPO beam edge to corner of rail, (b) couch is not modeled in TPS, manual extension of RPO beam edge along with use of ruler tool to define inner corner of couch rail (not seen in CT).

couch using the ruler or line drawing tool. Another line is drawn from the midline of the couch to the known location of the inside aspect of the right side rail. From that line, a third line is drawn downward from the surface of the couch representing the height of the rail. Now, the location of the inner posterior-most corner of the rail has been plotted and the edge of the RPO beam can be positioned to avoid it (white arrow). This simple method works for situations where attenuating couch structure geometry is relatively simple and well known. The choice of rail position must be determined by the radiotherapy team through discussion of the various options, such as patient-specific positions, fixed position for all patients with either beam avoidance or inclusion of the rails in the planning process, and the quality assurance implications of each.

When one is uncertain as to whether a beam passes through an attenuating external structure, then a portal image of that beam should be carefully reviewed to answer this question. Figure 15(a) shows a PA MV portal image (superior half of field) of a long posterior beam with a large collimator angle used to treat the femur in the frog-legged position, causing the beam to pass through the solid frame of the couch top. Figure 15(b) shows what this would look like if the plan had included the couch and frame structure. Indeed, one can see that the planning process would have predicted that the beam would pass through the couch top frame. This situation is not always
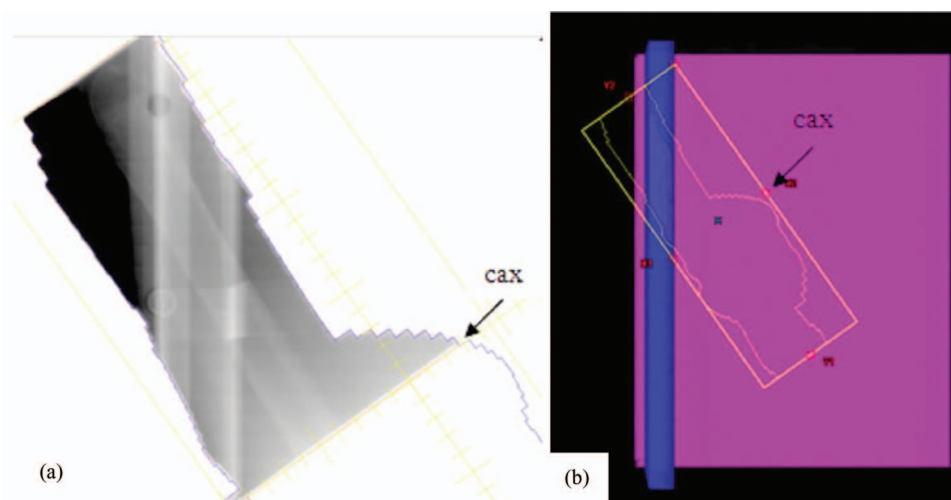
FIG. 15. (a) EPID image showing couch rail in beam. (b) Rail in beam modeled in TPS.

avoidable and in such cases an estimate of the dosimetric attenuation of the frame should be made. If the planning system is used to include the couch structure in the calculation, then this dose effect will be readily seen. In cases where the dose decrement is 5% or greater, the external device dose modeling has been validated, the patient is indexed and the daily reproducibility of patient position will be assured, one can add a subfield to the plan to boost the dose back to 100% just in the region of the attenuating structure.

5.B. Immobilization device avoidance

Some TPSs disallow dose calculations to any structure outside the patient body contour even if it were contoured and some do not allow bifurcated body contours, which stops the user from contouring the immobilization device as additional "body" volume. However, modern TPSs generally allow contouring and naming any pixel as part of the body contour and will then calculate the dose accordingly. Due to the greater uncertainty in the calculation, avoidance of more attenuating portions of immobilization devices may be wise even if the TPS includes them in the dose calculation.

Visualization and avoidance of immobilization devices is usually straightforward since these devices should always be in the planning CT images. Truncation of these devices from the image due to a small field of view should be avoided but is not always possible, for example, in the case of wing boards for breast treatment. In such cases, the immobilization device, if indexed, should be placed in the treatment position before the first treatment and the light field for each beam of the plan visualized for intersection with the device. The BEV feature in the TPS can be used to determine beam angles which avoid dense structures. An example of a head fixation system used for brain treatments is shown in Figs. 16(a) and 16(b). In the upper figure, the BEV shows the vertical post of the head fixation system overlapping with the PTV (red), causing the beam to pass through this attenuating structure. By rotating the gantry and/or couch, one can

visualize when the beam misses that structure. This example highlights the importance of contouring external structures so that one can take advantage of this BEV method of external structure avoidance. This approach is also useful for VMAT treatments where a portion or portions of an arc can be excluded which would otherwise traverse dense external structures. Proton planning demands that beam angles are chosen that avoid external devices that could result in abrupt WET changes.
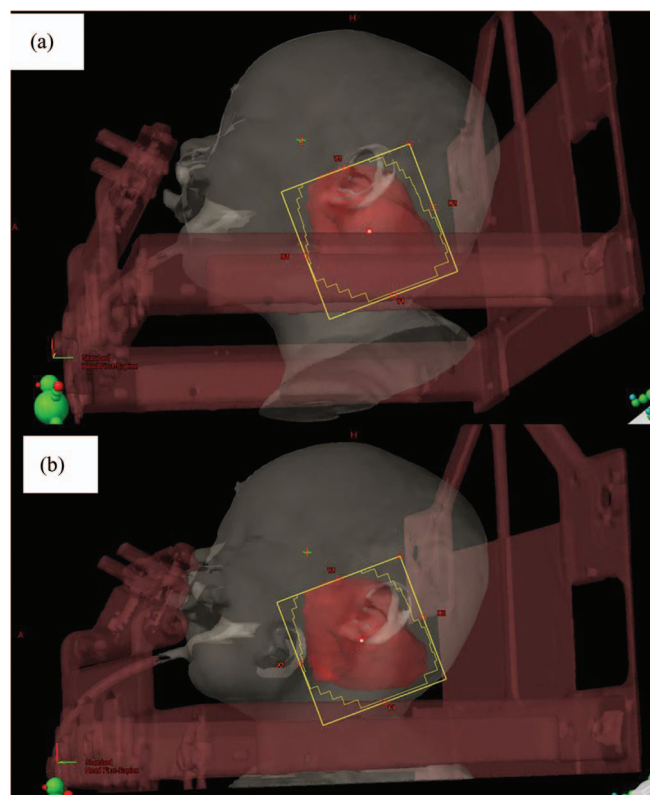

FIG. 16. (a) BEV of beam intersecting vertical post of immobilization device. (b) Gantry angle changed to avoid the post.

6. RECOMMENDATIONS TO TPS AND COUCH TOP VENDORS AND PHYSICISTS

6.A. Recommendations to TPS and couch top vendors

To improve the accuracy of dose calculations in the presence of external devices:

i.   The TPS should have models of the common couch tops from all vendors in the software which can be placed under the patient for indexed patients. The couch models should include all components such as rails and other structures.

ii. The TPS should allow models of the user's immobilization devices to be stored in a library in the software so they can be placed onto the patient CT planning images for indexed patients. This will facilitate contouring of these structures, especially when the device was partially obscured by a reduced field-of-view. Increasing the field-of-view may be necessary to accommodate this feature for both couch tops and immobilization devices.

iii. In the absence of the above two features, the TPS should allow the user to draw in or otherwise include any external structure (couch top or immobilization device) and include it in the calculations (again most useful for the indexed patient).

iv. The manufacturers of couch tops should supply technical drawings with dimensions and material composition to the TPS vendors.

v.   TPS vendors should quantify the accuracy of their couch models, i.e., calculate doses and compare to measurements for simple geometries.

vi. Couch top vendors should supply measured attenuation and WET data for their devices following the methods in Secs. 4.C and 4.D.

6.B. Recommendations to the physicist

For linac couch tops that are not present on the CT simulator, take steps to include a model of the couch top in the planning system. There are two basic approaches to include couch tops in the TPS: (a) by registering a CT scan of the treatment couch to the patient imaging study used for planning, and (b) create a contour model of the treatment couch, which combined with the appropriate physical or electron densities can be inserted in the patient imaging study for treatment planning. In either case:

i.   CT scan the linac couch top. This will tell you where the areas of nonuniform density or highly dense areas are. Metal plates integrated into the couch top for structural support may be present in areas through which beams can pass but their presence is not always obvious. Performing this CT scan is most feasible at the time of couch top installation. If CT scanning the linac couch top is not feasible, it can be surveyed radiographically by kV or MV imaging.

ii. Care must be taken to include in the TPS model the entire couch top that could potentially be in the treatment region if the couch top structure changes longitudinally.

iii. Daily reproducibility of the patient's position within the indexed system and the system's location relative to isocenter must be assured within tolerances established at the time of treatment planning.

iv. Measurements should be taken to validate the bulk densities and dimensions of the contoured models of the couch top.

v.   Measurements should be made to verify the planning system calculations and vendor supplied data for each type of device.

vi. Avoid the nonuniform and most attenuating portions if possible during the planning process and verify the adjustable parts (rails) are parked at the intended position during treatment.

If it is not possible to make a model of the couch top in the planning system:

i.   Measurements need to be taken to define the dose attenuation and surface dose at relevant locations for a range of beam directions. The method in Sec. 4.A. should be used.

ii. Alternatively, avoidance strategies should be determined to minimize the potential for beams to pass through the structure, at least for the higher density portions.

For immobilization devices (which should always be fully within the CT field of view), the device should be contoured as completely as possible for each case. If possible, the CT numbers resulting from the scan should be used rather than assigning a bulk density. The CT vs relative electron density table for the scanner should be in the planning system and validated. In cases where there are artifacts in the CT image of the immobilization system, bulk density values should be used to over-ride the artifact. Measurements should be made to verify the planning system calculations for each type of device.

7. SUMMARY AND CONCLUSIONS

Couch tops, immobilization devices, and combinations of such equipment can have a significant impact on patient dosimetry. While being light and rigid and providing artifact free cone beam CT as well as planar kV images, carbon fiber couch tops and immobilization devices can significantly alter the dose to the patient. All such devices have an associated radiological thickness and act as a bolus material, increasing skin dose while decreasing dose at depth. Attenuation through carbon fiber couch tops range from about 2% for normally incident beams through the central uniform portion to about 6% for highly oblique beams and can reach as much as 17% for more dense sections. These values increase with the combination of the couch top and immobilization device

(Table II) and skin doses can reach 100% of dose maximum (Table I).

Simplistic correction methods for couch attenuation may lead to an over- or underdose of part of the treatment volume. Manual alteration of TPS generated monitor units also risks transcription errors in the patient treatment plan. Modern treatment planning systems are generally capable of accurate and reliable dose calculations in the presence of patient immobilization devices. It has also been shown that various methods of couch incorporation into the treatment planning process can result in acceptable dose calculation accuracy. We recommend that TPS vendors automate this process and provide information for at least the most common couch tops. With the advent of VMAT, where a portion of the dose is almost always being delivered through posterior oblique angles, there is an increased interest in accounting for the presence of the couch top in the planning system. Incorporation of the couch top into proton beam planning systems is also recommended and can result in acceptable dose accuracy.

Measurement methods were described to assist the medical physicist in making measurements of attenuation and surface dose (or inference of surface dose from the WET and PDD) for external devices. These measurements serve to verify those supplied by the manufacturer and to validate the TPS modeling of those devices. Recommendations for measurement methods for manufacturers are given to provide consistency and transparency in reporting these values.

To avoid the need to modify or augment the planning CT images, it is strongly recommended that the same couch top be used for CT planning as for treatment and that a large enough field of view be utilized to encompass the full width of the couch top. For those who do not have dual couch tops (or in situations where the entire couch top is not included in the FOV), the TPS should provide the ability to position an accurate outline and assign appropriate densities of commonly available couch tops superimposed on the planning CT so that they can be included in the dose calculations. When it is not possible to include the treatment couch in the dose calculation, various methods were presented to avoid beam angles which would traverse highly attenuating external structures. Even if the TPS were capable of inclusion of the treatment couch top into the planning CT and dose calculation, it may be wise to simply avoid beams passing through the more attenuating sections.

ACKNOWLEDGMENTS

APPENDIX: ELECTRONIC SUPPLEMENT

Chamber	Window material	Window thickness gm/cm²	Collector	Collector diameter mm	Electrode separation mm	Wall material	Guard ring width mm	Reference
PTW 30–329 (Markus)	Polyethylene with graphite electrode	2.7	Graphite on polystyrene	5.4	2		0.3	Gerbi (Ref. 83)
Capintec PS-033	Mylar (aluminized)	0.0005	Carbon impregnated Shonka C552	16.2	2.4	polystyrene	2.5	Capintec catalog
ATTIX (RMI 449)	Graphite loaded Kapton	0.0048	Graphited Polyethylene	12.7	1	Solid water	13.5	IAEA TRS 381
PPC05 (IBA)	Shonka C552	0.176	PEEK graphite	9.9	0.6	Shonka C552	3.5	IBA spec
PPC40	PMMA	0.118	PMMA graphited	16	2	PMMA	4	IBA spec
IBA NACP	Mylar and graphite	0.104	PMMA graphited	10	2	PMMA	3	IBA spec
ROOS chamber PTW 34001	PMMA graphite coated	0.119	PMMA graphite coated	15	2	Acrylic	4	PTW spec sheet
Markus – Exradin A10	Kapton film	0.00386	Shonka C552	5.4	2	Shonka C552	4.3	Exradin spec sheet
Spokas – Exradin A11	Shonka C552	0.176	Shonka C552	20	2	Shonka C552	4.4	Exradin spec sheet
Spokas – Exradin A11TW	Kapton	0.00386	Shonka	20	3	Shonka	4.4	
Markus 23343 PTW	Polyethylene foil (graphited)	0.102	Polystyrene (graphited)	5.3	2	Polyethylene	0.2	
NACP01 Scandatronix	Graphite	0.09	Rexolite(graphited)	10	2	Graphite and rexolite	3	IAEA TRS 381
NACP02 Scandatronix	Mylar foil and graphite	0.104	Rexolite(graphited)	10	2	Graphite and rexolite	3	IAEA TRS 381

a)Author to whom correspondence should be addressed. Electronic mail: aolch@chla.usc.edu

[1]B. J. Mijnheer, J. J. Battermann, and A. Wambersie, "What degree of accuracy is required and can be achieved in photon and neutron therapy?," Radiother. Oncol. **8**, 237–252 (1987).

[2]A. Brahme, "Dosimetric precision requirements in radiation therapy," Acta Radiol.: Oncol. **23**, 379–391 (1984).

[3]S. Bentzen, "High-tech in radiation oncology: should there be a ceiling?," Int. J. Radiat. Oncol., Biol., Phys. **58**, 320–330 (2004).

[4]P. R. Almond, P. J. Biggs, B. M. Coursey, W. F. Hanson, M. S. Huq, R. Nath, and D. W. Rogers, "AAPM's TG-51 protocol for clinical reference dosimetry of high-energy photon and electron beams," Med. Phys. **26**, 1847–1870 (1999).

[5]L. G. de Mooy, "The use of carbon fibres in radiotherapy," Radiother. Oncol. **22**, 140–142 (1991).

[6]J. K. H. Seppälä and J. A. J. Kulmala, "Increased beam attenuation and surface dose by different couch inserts of treatment tables used in megavoltage radiotherapy," J. Appl. Clin. Med. Phys. **12**, 15–23 (2011).

[7]P. M. Mondalek, "Transmission and build up characteristics of polyurethane foam immobilization devices," Treat. Plann. **7**, 5–10 (1982).

[8]E. Vanetti, G. Nicolini, A. Clivio, A. Fogliata, and L. Cozzi, "The impact of treatment couch modelling on RapidArc," Phys. Med. Biol. **54**, N157–N166 (2009).

[9]K. B. Pulliam, R. M. Howell, D. Followill, D. Luo, R. A. White, and S. F. Kry, "The clinical impact of the couch top and rails on IMRT and arc therapy," Phys. Med. Biol. **56**, 7435–7447 (2011).

[10]T. Teke, B. Gill, C. Duzenli, and I. A. Popescu, "A Monte Carlo model of the Varian IGRT couch top for RapidArc QA," Phys. Med. Biol. **56**, N295–N305 (2011).

[11]E. Spezi, A. L. Angelini, F. Romani, A. Guido, F. Bunkheila, M. Ntreta, and A. Ferri, "Evaluating the influence of the Siemens IGRT carbon fibre tabletop in head and neck IMRT," Radiother. Oncol. **89**, 114–122 (2008).

[12]Z. Hu, J. Dai, L. Li, Y. Cao, and G. Fu, "Evaluating and modeling of photon beam attenuation by a standard treatment couch," J. Appl. Clin. Med. Phys. **12**, 139–146 (2011).

[13]L. H. Gerig, M. Niedbala, and B. J. Nyiri, "Dose perturbations by two carbon fiber treatment couches and the ability of a commercial treatment planning system to predict these effects," Med. Phys. **37**, 322–328 (2010).

[14]I. B. Mihaylov, P. Corry, Y. Yan, V. Ratanatharathorn, and E. G. Moros, "Modeling of carbon fiber couch attenuation properties with a commercial treatment planning system," Med. Phys. **35**, 4982–4988 (2008).

[15]J. O. Archambeau, R. Pezner, and T. Wasserman, "Pathophysiology of irradiated skin and breast," Int. J. Radiat. Oncol., Biol., Phys. **31**, 1171–1185 (1995).

[16]B. S. Hoppe, B. Laser, A. V. Kowalski, S. C. Fontenla, E. Pena-Greenberg, E. D. Yorke, D. M. Lovelock, M. A. Hunt, and K. E. Rosenzweig, "Acute skin toxicity following stereotactic body radiation therapy for stage I non-small-cell lung cancer: who's at risk?," Int. J. Radiat. Oncol., Biol., Phys. **72**, 1283–1286 (2008).

[17]S. F. Kry, S. A. Smith, R. Weathers, and M. Stovall, "Skin dose during radiotherapy: a summary and general estimation technique," J. Appl. Clin. Med. Phys. **13**, 20–34 (2012).

[18]B. De Ost, J. Vanregemorter, B. Schaeken, and D. Van den Weyngaert, "The effect of carbon fibre inserts on the build-up and attenuation of high energy photon beams," Radiother. Oncol. **45**, 275–277 (1997).

[19]D. M. Higgins, P. Whitehurst, and A. M. Morgan, "The effect of carbon fiber couch inserts on surface dose with beam size variation," Med. Dosim. **26**, 251–254 (2001).

[20]L. Court, J. Urribarri, and M. Makrigiorgos, "Carbon fiber couches and skin sparing," J. Appl. Clin. Med. Phys. **11**, 3241 (2010).

[21]S. McCormack, J. Diffey, and A. Morgan, "The effect of gantry angle on megavoltage photon beam attenuation by a carbon fiber couch insert," Med. Phys. **32**, 483–487 (2005).

[22]E. Spezi and A. Ferri, "dosimetric characteristics of the siemens IGRT carbon fiber tabletop," Med. Dosim. **32**, 295–298 (2007).

[23]M. Berg, J. P. Bangsgaard, and I. S. Vogelius, "Absorption measurements on a new cone beam CT and IMRT compatible tabletop for use in external radiotherapy," Phys. Med. Biol. **54**, N319–N328 (2009).

[24]M. J. Butson, T. Cheung, P. K. Yu, M. J. Butson, T. Cheung, and P. K. N. Yu, "Megavoltage x-ray skin dose variation with an angle using grid carbon fibre couch tops," Phys. Med. Biol. **52**, N485–N492 (2007).

[25]M. J. Butson, T. Cheung, P. K. Yu, P. Metcalfe, M. J. Butson, T. Cheung, P. K. N. Yu, and P. Metcalfe, "Measurement of skin dose variations produced by a silicon-based protective dressing in radiotherapy," Phys. Med. Biol. **47**, N145–N151 (2002).

[26]J. T. Whitton, "New values for epidermal thickness and their importance," Health Phys. **24**, 1–8 (1973).

[27]ICRU, "Recommendations of the International Commission on Radiological Protection," Ann. ICRP **21**, 1–201 (1991).

[28]International Commission on Radiation Units, "Dose and volume specification for reporting intracavitary therapy in gynaecology," ICRU Report 38 (ICRU Publications, Bethesda, MD, 1985).

[29]J. Carl and A. Vestergaard, "Skin damage probabilities using fixation materials in high-energy photon beams," Radiother. Oncol. **55**, 191–198 (2000).

[30]S. C. King, J. C. Acker, P. S. Kussin, L. B. Marks, K. J. Weeks, and K. A. Leopold, "High-dose, hyperfractionated, accelerated radiotherapy using a concurrent boost for the treatment of nonsmall cell lung cancer: Unusual toxicity and promising early results," Int. J. Radiat. Oncol., Biol., Phys. **36**, 593–599 (1996).

[31]N. Lee, C. Chuang, J. M. Quivey, T. L. Phillips, P. Akazawa, L. J. Verhey, and P. Xia, "Skin toxicity due to intensity-modulated radiotherapy for head-and-neck carcinoma," Int. J. Radiat. Oncol., Biol., Phys. **53**, 630–637 (2002).

[32]T. Meydanci and G. Kemikler, "Effect of a carbon fiber tabletop on the surface dose and attenuation for high-energy photon beams," Radiat. Med. **26**, 539–544 (2008).

[33]A. Gray, L. D. Oliver, and P. N. Johnston, "The accuracy of the pencil beam convolution and anisotropic analytical algorithms in predicting the dose effects due to attenuation from immobilization devices and large air gaps," Med. Phys. **36**, 3181–3191 (2009).

[34]I. B. Mihaylov, K. Bzdusek, and M. Kaus, "Carbon fiber couch effects on skin dose for volumetric modulated arcs," Med. Phys. **38**, 2419–2423 (2011).

[35]G. Krithivas and S. N. Rao, "Arc therapy dose perturbation due to the center bar in a Clinac 4/100 couch assembly," Med. Dosim. **13**, 15–18 (1988).

[36]S. C. Sharma and M. W. Johnson, "Photon beam attenuation for a patient support assembly during arc therapy for a medical linear accelerator," Med. Dosim. **17**, 225–228 (1992).

[37]W. K. Myint, M. Niedbala, D. Wilkins, and L. H. Gerig, "Investigating treatment dose error due to beam attenuation by a carbon fiber tabletop," J. Appl. Clin. Med. Phys. **7**, 21–27 (2006).

[38]S. Gillis, S. Bral, C. De Wagter, C. Derie, L. Paelinck, K. Van Vaerenbergh, M. Coghe, G. De Meerleer, and W. De Neve, "Evaluation of the Sinmed Mastercouch® as replacement for a standard couch," Radiother. Oncol. **75**, 227–236 (2005).

[39]R. A. Popple, J. B. Fiveash, I. A. Brezovich, and J. A. Bonner, "RapidArc radiation therapy: first year experience at the University of Alabama at Birmingham," Int. J. Radiat. Oncol., Biol., Phys. **77**, 932–941 (2010).

[40]H. Li, A. K. Lee, J. L. Johnson, R. X. Zhu, and R. J. Kudchadker, "Characterization of dose impact on IMRT and VMAT from couch attenuation for two Varian couches," J. Appl. Clin. Med. Phys. **12**, 23–31 (2011).

[41]M. Van Prooijen, T. Kanesalingam, M. K. Islam, and R. K. Heaton, "Assessment and management of radiotherapy beam intersections with the treatment couch," J. Appl. Clin. Med. Phys. **11**, 128–139 (2010).

[42]I. S. Grills, G. Hugo, L. L. Kestin, A. P. Galerani, K. K. Chao, J. Wloch, and D. Yan, "Image-guided radiotherapy via daily online cone-beam CT substantially reduces margin requirements for stereotactic lung radiotherapy," Int. J. Radiat. Oncol., Biol., Phys. **70**, 1045–1056 (2008).

[43]R. L. Rotondo, K. Sultanem, I. Lavoie, J. Skelly, and L. Raymond, "Comparison of repositioning accuracy of two commercially available immobilization systems for treatment of head-and-neck tumors using simulation computed tomography imaging," Int. J. Radiat. Oncol., Biol., Phys. **70**, 1389–1396 (2008).

[44]M. W. Johnson, M. A. Griggs, and S. C. Sharma, "A comparison of surface doses for two immobilizing systems," Med. Dosim. **20**, 191–194 (1995).

[45]D. E. Mellenberg, "Dose Behind Various Immobilization and Beam-Modifying Devices," Int. J. Radiat. Oncol., Biol., Phys. **32**, 1193–1197 (1995).

[46]T. Cheung, M. J. Butson, and P. K. N. Yu, "Evaluation of build-up dose from 6 MV X-rays under pelvic and abdominal patient immobilisation devices," Radiat. Measur. **35**, 235–238 (2002).

[47]K. W. Lee, J. K. Wu, S. C. Jeng, Y. W. Hsueh Liu, and J. C. Cheng, "Skin dose impact from vacuum immobilization device and carbon fiber couch in intensity modulated radiation therapy for prostate cancer," Med. Dosim. **34**, 228–232 (2009).

[48]S. J. Meara and K. A. Langmack, "An investigation into the use of carbon fibre for megavoltage radiotherapy applications," Phys. Med. Biol. **43**, 1359–1366 (1998).

[49]A. J. Olch and R. S. Lavey, "Reproducibility and treatment planning advantages of a carbon fiber relocatable head fixation system," Radiother. Oncol. **65**, 165–168 (2002).

[50]S. W. Hadley, R. Kelly, and K. Lam, "Effects of immobilization mask material on surface dose," J. Appl. Clin. Med. Phys. **6**, 1–7 (2005).

[51]E. A. Halm, A. Tamri, A. Bridier, P. Wibault, and F. Eschwege, "[Influence of thermoplastic masks on the absorbed skin dose for head and neck tumor radiotherapy]," Cancer Radiother. **6**, 310–319 (2002).

[52]D. P. Fontenla, J. J. Napoli, M. Hunt, D. Fass, B. McCormick, and G. J. Kutcher, "Effects of beam modifiers and immobilization devices on the dose in the build-up region," Int. J. Radiat. Oncol., Biol., Phys. **30**, 211–219 (1994).

[53]C. Fiorino, G. M. Cattaneo, A. Delvecchio, M. Fusca, B. Longobardi, P. Signorotto, and R. Calandrino, "Skin-sparing reduction effects of thermoplastics used for patient immobilization in head and neck radiotherapy," Radiother. Oncol. **30**, 267–270 (1994).

[54]A. Kelly, N. Hardcastle, P. Metcalfe, D. Cutajar, A. Quinn, M. Cardoso, S. Barlin, and A. Rosenfeld, "Surface dosimetry for breast radiotherapy in the presence of immobilization cast material," Phys. Med. Biol. **56**, 1001–1013 (2011).

[55]B. Poppe, N. Chofor, A. Ruhmann, W. Kunth, A. Djouguela, R. Kollhoff, and K. C. Willborn, "The effect of a carbon-fiber couch on the depth-dose curves and transmission properties for megavoltage photon beams," Strahlenther. Onkol. **183**, 43–48 (2007).

[56]S.-T. Chiu-Tsao and M. F. Chan, "Evaluation of two-dimensional bolus effect of immobilization/support devices on skin doses: A radiochromic EBT film dosimetry study in phantom," Med. Phys. **37**, 3611–3620 (2010).

[57]R. K. Munjal, P. S. Negi, A. G. Babu, S. N. Sinha, A. K. Anand, and T. Kataria, "Impact of 6 MV photon beam attenuation by carbon fiber couch and immobilization devices in IMRT planning and dose delivery," J. Med. Phys. **31**, 67–71 (2006).

[58]C. F. Njeh, T. W. Raines, and M. W. Saunders, "Determination of the photon beam attenuation by the Brainlab imaging couch: angular and field size dependence," J. Appl. Clin. Med. Phys. **10**, 16–27 (2009).

[59]S. J. Becker, G. Jozsef, and J. K. DeWyngaert, "Characterization of the transmission of the Elekta Stereotactic Body Frame (ESBF) and accounting for it during treatment planning," Med. Dosim. **34**, 154–157 (2009).

[60]J. Pouliot, B. Werner, J. Riley, M. Herron, S. Dimmer, J. Wright, and T. Mate, "Demonstration of minimal impact to radiation beam and portal image quality due to the presence of an electromagnetic array," Med. Phys. **30**, 1473–1473 (2003).

[61]S. Li and C. Enke, "Dosimetry impact of radiation beams due to presence of calypso electromagnetic array," Med. Phys. **35**, 2852–2852 (2008).

[62]A. Kassaee, L. Lin, E. Garver, J. Metz, and N. Vapiwala, "Beam attenuation and beam spoiling properties of an electromagnetic array used for patient localization and tumor tracking," Med. Phys. **36**, 2601–2602 (2009).

[63]L. Santanam, C. Noel, T. R. Willoughby, J. Esthappan, S. Mutic, E. E. Klein, D. A. Low, and P. J. Parikh, "Quality assurance for clinical implementation of an electromagnetic tracking system," Med. Phys. **36**, 3477–3486 (2009).

[64]M. Yoon, J. Kim, S. Ahn, M. Cheong, Y. Lim, D. Kim, D. Shin, S. Lee, and S. Park, "Study on the modeling of digital couch for proton treatment planning system," Med. Phys. **36**, 2632–2633 (2009).

[65]Z. Yu, J. Bluett, Y. Zhang, X. Zhu, M. Lii, R. Mohan, and L. Dong, "Impact of daily patient setup variation on proton beams passing through the couch edge," Med. Phys. **37**, 3294–3294 (2010).

[66]D. W. Smith, D. Christophides, C. Dean, M. Naisbit, J. Mason, and A. Morgan, "Dosimetric characterization of the iBEAM evo carbon fiber couch for radiotherapy," Med. Phys. **37**, 3595–3606 (2010).

[67]I. B. Mihaylov, J. Penagaricano, and E. G. Moros, "Quantification of the skin sparing effect achievable with high-energy photon beams when carbon fiber tables are used," Radiother. Oncol. **93**, 147–152 (2009).

[68]D. Wagner and H. Vorwerk, "Treatment modeling in the treatment planning system eclipse," J. Cancer Sci. **3**, 188–193 (2011).

[69]U. Schneider, E. Pedroni, and A. Lomax, "The calibration of CT Hounsfield units for radiotherapy treatment planning," Phys. Med. Biol. **41**, 111–124 (1996).

[70]M. F. Moyers, M. Sardesai, S. Sun, and D. W. Miller, "Ion stopping powers and CT numbers," Med. Dosim. **35**, 179–194 (2010).

[71]M. F. Moyers and D. W. Miller, "Range, range modulation, and field radius requirements for proton therapy of prostate cancer," Technol. Cancer Res. Treat. **2**, 445–447 (2003).

[72]M. F. Moyers, D. W. Miller, D. A. Bush, and J. D. Slater, "Methodologies and tools for proton beam design for lung tumors," Int. J. Radiat. Oncol., Biol., Phys. **49**, 1429–1438 (2001).

[73]S. C. Vieira, R. S. Kaatee, M. L. Dirkx, and B. J. Heijmen, "Two-dimensional measurement of photon beam attenuation by the treatment couch and immobilization devices using an electronic portal imaging device," Med. Phys. **30**, 2981–2987 (2003).

[74]A. S. A. M. Ali, M. L. P. Dirkx, M. G. J. Breuers, and B. J. M. Heijmen, "Inclusion of the treatment couch in portal dose image prediction for high precision EPID dosimetry," Med. Phys. **38**, 377–381 (2011).

[75]A. Mans, P. Remeijer, I. Olaciregui-Ruiz, M. Wendling, J. J. Sonke, B. Mijnheer, M. van Herk, and J. C. Stroom, "3D dosimetric verification of volumetric-modulated arc therapy by portal dosimetry," Radiother. Oncol. **94**, 181–187 (2010).

[76]J. Chen, C. F. Chuang, O. Morin, M. Aubin, and J. Pouliot, "Calibration of an amorphous-silicon flat panel portal imager for exit-beam dosimetry," Med. Phys. **33**, 584–594 (2006).

[77]P. B. Greer, "Correction of pixel sensitivity variation and off-axis response for amorphous silicon EPID dosimetry," Med. Phys. **32**, 3558–3568 (2005).

[78]C. Kirkby and R. Sloboda, "Consequences of the spectral response of an a-Si EPID and implications for dosimetric calibration," Med. Phys. **32**, 2649–2658 (2005).

[79]S. L. Berry, C. S. Polvorosa, and C. S. Wuu, "A field size specific backscatter correction algorithm for accurate EPID dosimetry," Med. Phys. **37**, 2425–2434 (2010).

[80]W. van Elmpt, L. McDermott, S. Nijsten, M. Wendling, P. Lambin, and B. Mijnheer, "A literature review of electronic portal imaging for radiotherapy dosimetry," Radiother. Oncol. **88**, 289–309 (2008).

[81]H. A. Hughes, "Measurements of superficial absorbed dose with 2 MV x rays used at glancing angles," Br. J. Radiol. **32**, 255–258 (1959).

[82]S. Kim, C. R. Liu, T. C. Zhu, and J. R. Palta, "Photon beam skin dose analyses for different clinical setups," Med. Phys. **25**, 860–866 (1998).

[83]B. J. Gerbi, "The response characteristics of a newly designed plane-parallel ionization chamber in high-energy photon and electron beams," Med. Phys. **20**, 1411–1415 (1993).

[84]W. Abdel-Rahman, J. P. Seuntjens, F. Verhaegen, F. Deblois, and E. B. Podgorsak, "Validation of Monte Carlo calculated surface doses for megavoltage photon beams," Med. Phys. **32**, 286–298 (2005).

[85]S. Devic, J. Seuntjens, W. Abdel-Rahman, M. Evans, M. Olivares, E. B. Podgorsak, T. Vuong, and C. G. Soares, "Accurate skin dose measurements using radiochromic film in clinical applications," Med. Phys. **33**, 1116–1124 (2006).

[86]N. Dogan and G. P. Glasgow, "Surface and build-up region dosimetry for obliquely incident intensity modulated radiotherapy 6 MV x rays," Med. Phys. **30**, 3091–3096 (2003).

[87]B. J. Gerbi and F. M. Khan, "Plane-parallel ionization chamber response in the buildup region of obliquely incident photon beams," Med. Phys. **24**, 873–878 (1997).

[88]S. Stathakis, J. S. Li, K. Paskalev, J. Yang, L. Wang, and C. M. Ma, "Ultra-thin TLDs for skin dose determination in high energy photon beams," Phys. Med. Biol. **51**, 3549–3567 (2006).

[89]D. A. Low, J. M. Moran, J. F. Dempsey, L. Dong, and M. Oldham, "Dosimetry tools and techniques for IMRT," Med. Phys. **38**, 1313–1338 (2011).

[90]B. Nilsson and A. Montelius, "Fluence perturbation in photon beams under nonequilibrium conditions," Med. Phys. **13**, 191–195 (1986).

[91]G. Failla, "Measurement of tissue dose in terms of the same unit for all ionizing radiation," Radiology **29**, 202–215 (1937).

[92]J. A. Rawlinson, D. Arlen, and D. Newcombe, "Design of parallel plate ion chambers for buildup measurements in megavoltage photon beams," Med. Phys. **19**, 641–648 (1992).

[93]D. E. Velkley, D. J. Manson, J. A. Purdy, and G. D. Oliver, Jr., "Build-up region of megavoltage photon radiation sources," Med. Phys. **2**, 14–19 (1975).

[94] C. E. Zankowski and E. B. Podgorsak, "Calibration of photon and electron beams with an extrapolation chamber," Med. Phys. **24**, 497–503 (1997).

[95] J. L. Howarth, J. C. Jones, and H. Miller, "Physical measurements on a 2 MeV. X-ray generator," Br. J. Radiol. **24**, 665–675 (1951).

[96] T. Kron, A. Elliot, T. Wong, G. Showell, B. Clubb, and P. Metcalfe, "X-ray surface dose measurements using TLD extrapolation," Med. Phys. **20**, 703–711 (1993).

[97] M. Budanec, Z. Knezevic, T. Bokulic, I. Mrcela, M. Vrtar, B. Vekic, and Z. Kusic, "Comparison of doses calculated by the Monte Carlo method and measured by LiF TLD in the buildup region for a 60Co photon beam," Appl. Radiat. Isot. **66**, 1925–1929 (2008).

[98] P. Rapley, "Surface dose measurement using TLD powder extrapolation," Med. Dosim. **31**, 209–215 (2006).

[99] S. J. Thomas and N. Palmer, "The use of carbon-loaded thermoluminescent dosimeters for the measurement of surface doses in megavoltage x-ray beams," Med. Phys. **16**, 902–904 (1989).

[100] J. R. Greening, "The photographic action of x-rays," Proc. Phys. Soc. **64**, 977–992 (1951).

[101] M. Butson, "Radiochromic film as a radiotherapy surface-dose detector," Phys. Med. Biol. **41**, 1073–1078 (1996).

[102] S. Pai, I. J. Das, J. F. Dempsey, K. L. Lam, T. J. Losasso, A. J. Olch, J. R. Palta, L. E. Reinstein, D. Ritt, and E. E. Wilcox, "TG-69: radiographic film for megavoltage beam dosimetry," Med. Phys. **34**, 2228–2258 (2007).

[103] M. J. Butson, T. Cheung, P. K. N. Yu, and M. Currie, "Surface dose extrapolation measurements with radiographic film," Phys. Med. Biol. **49**, N197–N201 (2004).

[104] A. Niroomand-Rad, C. R. Blackwell, B. M. Coursey, K. P. Gall, J. M. Galvin, W. L. McLaughlin, A. S. Meigooni, R. Nath, J. E. Rodgers, and C. G. Soares, "Radiochromic film dosimetry: recommendations of AAPM Radiation Therapy Committee Task Group 55. American Association of Physicists in Medicine," Med. Phys. **25**, 2093–2115 (1998).

[105] M. J. Butson, P. K. N. Yu, and P. E. Metcalfe, "Extrapolated surface dose measurements with radiochromic film," Med. Phys. **26**, 485–488 (1999).

[106] S. T. Chiu-Tsao and M. F. Chan, "Photon beam dosimetry in the superficial buildup region using radiochromic EBT film stack," Med. Phys. **36**, 2074–2083 (2009).

[107] E. O'Shea and P. McCavana, "Review of surface dose detectors in radiotherapy," J. Radiother. Prac. **3**, 69–76 (2003).

[108] K. De Vlamynck, C. De Wagter, and W. De Neve, "Diamond detector measurements near simulated air channels for narrow photon beams," Radiother. Oncol. **53**, 155–159 (1999).

[109] C. De Angelis, S. Onori, M. Pacilio, G. A. Cirrone, G. Cuttone, L. Raffaele, M. Bucciolini, and S. Mazzocchi, "An investigation of the operating characteristics of two PTW diamond detectors in photon and electron beams," Med. Phys. **29**, 248–254 (2002).

[110] M. Bucciolini, F. B. Buonamici, S. Mazzocchi, C. De Angelis, S. Onori, and G. A. Cirrone, "Diamond detector versus silicon diode and ion chamber in photon beams of different energy and field size," Med. Phys. **30**, 2149–2154 (2003).

[111] C. Scherf, C. Peter, J. Moog, J. Licher, E. Kara, K. Zink, C. Rodel, and U. Ramm, "Silicon diodes as an alternative to diamond detectors for depth dose curves and profile measurements of photon and electron radiation," Strahlenther. Onkol. **185**, 530–536 (2009).

[112] M. Butson, "A new radiotherapy surface dose detector: The MOSFET," Med. Phys. **23**, 655–658 (1996).

[113] J. A. Snir, H. Mosalaei, K. Jordan, and S. Yartsev, "Surface dose measurement for helical tomotherapy," Med. Phys. **38**, 3104–3107 (2011).

[114] P. A. Jursinic, "Characterization of optically stimulated luminescent dosimeters, OSLDs, for clinical dosimetric measurements," Med. Phys. **34**, 4594–4604 (2007).

[115] M. S. Muthuswamy, "A method of beam-couch intersection detection," Med. Phys. **26**, 229–235 (1999).

[116] I. Beange and A. Nisbet, "A collision prevention software tool for complex three-dimensional isocentric set-ups," Br. J. Radiol. **73**, 537–541 (2000).

[117] A. H. Buckle, "An algorithm for detection of couch-beam intersection," Med. Dosim. **30**, 65–68 (2005).

[118] J. Meyer, J. A. Mills, O. C. L. Haas, K. J. Burnham, and E. M. Parvin, "Accommodation of couch constraints for coplanar intensity modulated radiation therapy," Radiother. Oncol. **61**, 23–32 (2001).